applied sciences

MDPI

Article

Analytical Modeling of Current-Voltage Photovoltaic Performance: An Easy Approach to Solar Panel Behavior

José Miguel Álvarez [1], Daniel Alfonso-Corcuera [1,2], Elena Roibás-Millán [1,2], Javier Cubas [1,2], Juan Cubero-Estalrrich [1], Alejandro Gonzalez-Estrada [1], Rocío Jado-Puente [1], Marlon Sanabria-Pinzón [1] and Santiago Pindado [1,2,*]

1 Instituto Universitario de Microgravedad "Ignacio Da Riva" (IDR/UPM), ETSI Aeronáutica y del Espacio, Universidad Politécnica de Madrid, Plaza del Cardenal Cisneros 3, 28040 Madrid, Spain; jm.alvarez@upm.es (J.M.Á.); daniel.alfonso.corcuera@upm.es (D.A.-C.); elena.roibas@upm.es (E.R.-M.); j.cubas@upm.es (J.C.); jl.cubero@alumnos.upm.es (J.C.-E.); alejandro.gonzalez.estrada@alumnos.upm.es (A.G.-E.); rocio.jado.puente@alumnos.upm.es (R.J.-P.); ms.sanabria@alumnos.upm.es (M.S.-P.)

2 Departamento de Sistemas Aeroespaciales, Transporte Aéreo y Aeropuertos (SATAA), ETSI Aeronáutica y del Espacio, Universidad Politécnica de Madrid, Plaza del Cardenal Cisneros 3, 28040 Madrid, Spain

* Correspondence: santiago.pindado@upm.es

Abstract: In this paper, we propose very simple analytical methodologies for modeling the behavior of photovoltaic (solar cells/panels) using a one-diode/two-resistor (1-D/2-R) equivalent circuit. A value of $a = 1$ for the ideality factor is shown to be very reasonable for the different photovoltaic technologies studied here. The solutions to the analytical equations of this model are simplified using easy mathematical expressions defined for the Lambert W-function. The definition of these mathematical expressions was based on a large dataset related to solar cells and panels obtained from the available academic literature. These simplified approaches were successfully used to extract the parameters from explicit methods for analyzing the behavior of solar cells/panels, where the exact solutions depend on the Lambert W-function. Finally, a case study was carried out that consisted of fitting the aforementioned models to the behavior (that is, the *I-V* curve) of two solar panels from the UPMSat-1 satellite. The results show a fairly high level of accuracy for the proposed methodologies.

Keywords: solar cell; solar panel; parameter extraction; analytical; Lambert W-function; spacecraft solar panels; *I-V* curve; modeling

Citation: Álvarez, J.M.; Alfonso-Corcuera, D.; Roibás-Millán, E.; Cubas, J.; Cubero-Estalrrich, J.; Gonzalez-Estrada, A.; Jado-Puente, R.; Sanabria-Pinzón, M.; Pindado, S. Analytical Modeling of Current-Voltage Photovoltaic Performance: An Easy Approach to Solar Panel Behavior. *Appl. Sci.* **2021**, *11*, 4250. https://doi.org/10.3390/app11094250

Academic Editor: Luis Hernández-Callejo

Received: 13 March 2021
Accepted: 3 May 2021
Published: 7 May 2021

1. Introduction

Based on the installation of power plants over the last few decades, it can be seen that photovoltaic energy has emerged as a very important factor in policies relating to renewable energy sources [1–7]. As an energy source, solar panels have a significant competitive edge over other renewable energy sources due to their potential for dual-use at either the industrial or the domestic scale. Both possibilities have provided an impetus for the increasing growth in demand for photovoltaic systems [5,8–11].

Photovoltaic energy has also been demonstrated to be crucial for stand-alone power systems such as glow-in-the-dark lettering and illuminated signs on highways. One of the first such stand-alone industrial applications of photovoltaic technologies was in power generation in spacecraft. According to Rauschenbach, "The first solar cell array that successfully operated in space was launched on 17 March 1958, on board Vanguard I, the second U.S. earth satellite" [12].

Modeling the performance of power sub-systems for space missions is essential at the predesign stage. At these early configuration stages of a space mission, simple, fast simulations are required that are as accurate as possible. This trend has also been amplified by the increasing importance of Concurrent Design (CD) in industrial processes. According to the European Cooperation for Space Standardization (ECSS), CD is especially important in the early predesign phase of space missions. It is based on the parallelization of processes associated with different sub-systems and is carried out in a special working environment organized into Concurrent Design Facilities (CDFs), where design parameters are shared, and the information flow is organized thus that stable solutions can be reached as quickly as possible [13–17].

Research carried out at the IDR/UPM Institute on solar panels has been driven by the need for simple procedures to calculate the performance of these panels. This need has arisen in the context of mission predesign at the CDF [18,19], and particularly in relation to sub-system coupling effects, such as those that can be found when analyzing thermal control and power distribution in spacecraft.

The simulation of photovoltaic devices (solar cells/panels) is normally carried out by means of equivalent circuit models, which are defined by implicit mathematical expressions. However, problems arise in terms of:

- The extraction of the parameters appearing in this equation, which define the performance of the photovoltaic device at a certain temperature and irradiance level, and;
- The calculation of the output current as a function of the output voltage, or vice versa, since this equation is implicit.

There are multiple ways to fit the equation for the photovoltaic equivalent circuit models to experimental data [20–29]. All of these approaches can essentially be grouped into two different types: Numerical (in which the equation is fitted to a large dataset that represents the *I-V* curve of the photovoltaic device) and analytical (in which the parameters of the equation are extracted based on three points of the *I-V* curve: short circuit, maximum power, and open voltage).

The second issue described above, i.e., the calculation of the output current as a function of the output voltage once the parameters of the equation have been extracted, can only be solved by numerical approaches [30–46] (which include iterative solutions [47–49]), or by using of the Lambert W-function [50–55] (whose exact calculation requires a numerical approach).

Possible solutions to the aforementioned problems include explicit methods of photovoltaic modeling, which are based on explicit equations with parameters defined based on the characteristic points of the *I-V* curve. Some of these methods also require the use of the Lambert W-function to define the parameters [56].

In the present work, we explore two important aspects of the analytical approach to the one diode/two resistor (1-D/2-R) equivalent circuit model for solar panels:

- Selection of a proper ideality factor for extraction of the model parameters based on analytical methods, as this forms the cornerstone for extracting the other four parameters [57], and;
- Development of a simplified approach to the Lambert W-function, which is required in this analytical methodology in order to:
    - Obtain the value of the first parameter of the 1-D/2-R equivalent circuit model, i.e., the value of the resistance of the series-connected resistor, and;
    - Solve the implicit equation of this model to derive the output current in relation to the output voltage.

Our simplified approach to the Lambert W-function is also proven to be a relatively powerful tool for extracting the parameters of some of the most accurate explicit equations for photovoltaic modeling that can be found in the literature: the models of Kalmarlar and Haneefa [58,59] and Das [60].

The aim of this paper is to define very simple methodologies to measure the performance of photovoltaic devices (solar cells/panels), thus that these can be implemented as part of more complex simulations. One example of this type of simulation is the coupled thermo-electrical modeling of space systems with ESATAN© [61]. It should also be emphasized that these methodologies may be useful tools for professionals within small and medium-sized enterprises in the solar energy sector to allow them to estimate the performance of the systems they design. Additionally, the increasing use of photovoltaic generation in small grids [62,63] could increase the worth of the easy approximations to solar panels performance included in this paper.

This paper is organized as follows. A simple model of solar panels is described in Section 2, and simplified equations for solving the 1-D/2-R equivalent circuit model and the Lambert W-function are given in Section 3. A case study is also described and solved in Section 3, using the procedures described in the preceding sub-sections. Finally, conclusions are presented in Section 4.

2. Modeling of Photovoltaic Systems

2.1. The 1-D/2-R Equivalent Circuit Model

The most widely used method of modeling the performance of a solar cell/panel (based on its *I-V* curve, where I is the output current and V the output voltage) is an equivalent circuit based on one current source, one diode, and two resistors (series and shunt resistors), as shown in Figure 1. The equation that describes the performance of this model is as follows [57,64–66]:

$$I = I_{pv} - I_0 \left[\exp\left(\frac{V + IR_s}{naV_T} \right) - 1 \right] - \frac{V + IR_s}{R_{sh}} \tag{1}$$

where I_{pv} is the photocurrent, I_0 is the reverse saturation current of the diode, R_{sh} is the resistance of the shunt resistor, R_s is the resistance of the series-connected resistor, and V_T is the thermal voltage:

$$V_T = \frac{\kappa T}{q} \tag{2}$$

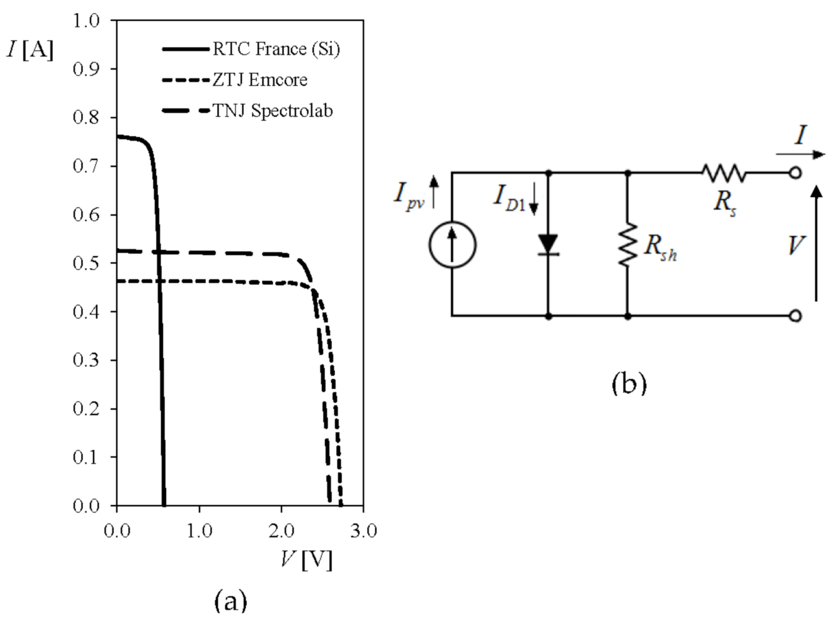

Figure 1. (**a**) *I-V* curves for three different solar cells; (**b**) 1-D/2-R equivalent circuit model for analyzing the behavior of a solar cell/panel.

In the above equation, $\kappa = 1.38064852 \cdot 10^{-23}$ m^2 kg s^{-2} K^{-1} is the Boltzmann constant, T is the temperature expressed in K, and $q = 1.60217662 \cdot 10^{-19}$ C is the electron charge. In Equation (1), a is the ideality factor of the diode (in principle, the effect of temperature on this parameter can be left aside [64]), and n is the number of series-connected cells in the solar panel (obviously, $n = 1$ when studying the performance of a single cell).

The first problem of modeling a photovoltaic device with the 1-D/2-R equivalent circuit model lies in extracting the five parameters of the model: I_{pv}, I_0, a, R_s, and R_{sh}. Depending on the available information, which might be either:

- The *I-V* curve with an enough large number of points, or;
- The three characteristic points of the *I-V* curve (short circuit output current, I_{sc}, open circuit output voltage, V_{oc}, and output current and voltage levels at the Maximum Power Point (MPP), I_{mp} and V_{mp},

It is possible to extract these five parameters either by numerically fitting Equation (1) to the *I-V* curve, or by using the three characteristic points, which in practice represent four conditions [67]: the first three of which force the equation to match the points (0, I_{sc}), (V_{mp}, I_{mp}) and (V_{oc}, 0), and the fourth is related to the maximum power condition:

$$-\left.\frac{\partial I}{\partial V}\right|_{(V_{mp},I_{mp})} = \frac{I_{mp}}{V_{mp}}. \tag{3}$$

Modeling the performance of photovoltaic systems with the equivalent circuit described here can be very advantageous, as these circuits somehow preserve the physical processes of a pair formed of a current source and a p-n junction [68]. The effect of the series-connected resistor, R_s, is mainly associated with power losses in the solder bonds and interconnections between cells, whereas the effect of the shunt resistor, R_{sh}, is associated with current leakages across the p-n junction [69,70]. In recent years, several reviews of the different procedures and techniques for the parameter extraction problem related to the 1-D/2-R model have been published [20,21,23,24,67,71–73]. The present work focuses on an analytical approach based on the use of information from the characteristic points to calculate the five parameters in Equation (1). The following equations can be derived [57]:

$$\frac{naV_T V_{mp}(2I_{mp} - I_{sc})}{(V_{mp}I_{sc} + V_{oc}(I_{mp} - I_{sc}))(V_{mp} - I_{mp}R_s) - naV_T(V_{mp}I_{sc} - V_{oc}I_{mp})} = \exp\left(\frac{V_{mp} + I_{mp}R_s - V_{oc}}{naV_T}\right), \tag{4}$$

$$R_{sh} = \frac{(V_{mp} - I_{mp}R_s)(V_{mp} - R_s(I_{sc} - I_{mp}) - naV_T)}{(V_{mp} - I_{mp}R_s)(I_{sc} - I_{mp}) - naV_T I_{mp}}, \tag{5}$$

$$I_{pv} = \frac{R_{sh} + R_s}{R_{sh}} I_{sc}, \tag{6}$$

$$I_0 = \frac{(R_{sh} + R_s)I_{sc} - V_{oc}}{R_{sh}\exp\left(\frac{V_{oc}}{naV_T}\right)}. \tag{7}$$

Three problems arise at this point:

- A sufficiently accurate estimation of the ideality factor a is required;
- Equation (4) is an implicit mathematical expression for solving R_s, and an iterative process is, therefore, required to extract this parameter; and
- Equation (1), which defines the performance of the solar cell/panel, is also an implicit expression. As a consequence, once all the parameters of this equation have been extracted, an additional iterative process will be required to solve it (i.e., to derive the value of the output current, I, for a given value of the output voltage level, V).

Fortunately, the ideality factor can be estimated by taking a value within the range from a = 1 to a = 1.5 [74,75], and the value of the resistance of the series-connected resistor, R_s, can be derived from [64]:

$$R_s = A(W_{-1}(B\exp(C)) - (D + C)), \tag{8}$$

where W_{-1} is the negative branch of the Lambert W-function (see Section 2.1). The variables A, B, C, and D are defined as:

$$A = \frac{naV_T}{I_{mp}}, \tag{9}$$

$$B = -\frac{V_{mp}\left(2I_{mp} - I_{sc}\right)}{V_{mp}I_{sc} + V_{oc}\left(I_{mp} - I_{sc}\right)}, \tag{10}$$

$$C = -\frac{2V_{mp} - V_{oc}}{naV_T} + \frac{V_{mp}I_{sc} - V_{oc}I_{mp}}{V_{mp}I_{sc} + V_{oc}\left(I_{mp} - I_{sc}\right)}, \tag{11}$$

$$D = \frac{V_{mp} - V_{oc}}{naV_T}. \tag{12}$$

However, the problem of solving the implicit equation in (1) still remains after the extraction of parameters a and R_s. Authors such as Peng et al. [50] have shown that this equation can also be solved using the Lambert W-function:

$$I = \frac{R_{sh}\left(I_{pv} + I_0\right) - V}{R_{sh} + R_s} - \frac{naV_T}{R_s} W_0\left(\frac{R_{sh}R_sI_0}{naV_T(R_{sh} + R_s)} \exp\left(\frac{R_{sh}R_s\left(I_{pv} + I_0\right) + R_{sh}V}{naV_T(R_{sh} + R_s)}\right)\right), \tag{13}$$

where W_0 is the positive branch of the Lambert W-function (see Section 2.1).

2.2. Explicit Equations/Models as Alternative to the 1-D/2-R Equivalent Circuit Model

The difficulties associated with solving the 1-D/2-R model implicit equation drove researchers to develop explicit equations for modeling the performance of solar cells/panels [58,59,76–82]. These photovoltaic models give the output current as a function of the output voltage by using simple mathematical models or equations that can be easily solved without the need for advanced mathematical tools. Of these, three models appear to be fairly accurate in relation to the *I-V* curve. The model proposed by Kalmarkar and Haneefa [58,59] is:

$$\frac{I}{I_{sc}} = 1 - (1-\gamma)\frac{V}{V_{oc}} - \gamma\left(\frac{V}{V_{oc}}\right)^m, \tag{14}$$

where [56]:

$$\gamma = \frac{2\left(\frac{I_{mp}}{I_{sc}}\right) - 1}{(m-1)\left(\frac{V_{mp}}{V_{oc}}\right)^m}, \tag{15}$$

$$m = \frac{W_{-1}\left(-\left(\frac{V_{oc}}{V_{mp}}\right)^{\frac{1}{K}}\left(\frac{1}{K}\right)\ln\left(\frac{V_{mp}}{V_{oc}}\right)\right)}{\ln\left(\frac{V_{mp}}{V_{oc}}\right)} + \frac{1}{K} + 1, \tag{16}$$

and:

$$K = \frac{1 - \left(\frac{I_{mp}}{I_{sc}}\right) - \left(\frac{V_{mp}}{V_{oc}}\right)}{2\left(\frac{I_{mp}}{I_{sc}}\right) - 1}, \tag{17}$$

the model proposed by Das [60] is:

$$\frac{I}{I_{sc}} = \frac{1 - \left(\frac{V}{V_{oc}}\right)^k}{1 + h\left(\frac{V}{V_{oc}}\right)}, \tag{18}$$

where [56]:

$$k = \frac{W_{-1}\left(\left(\frac{I_{mp}}{I_{sc}}\right)\ln\left(\frac{V_{mp}}{V_{oc}}\right)\right)}{\ln\left(\frac{V_{mp}}{V_{oc}}\right)}, \tag{19}$$

$$h = \left(\frac{V_{oc}}{V_{mp}}\right)\left(\frac{I_{sc}}{I_{mp}} - \frac{1}{k} - 1\right), \tag{20}$$

while the model of Pindado and Cubas [56,80] is:

$$I = \begin{cases} I_{sc}\left(1-\left(1-\frac{I_{mp}}{I_{sc}}\right)\left(\frac{V}{V_{mp}}\right)^{\frac{I_{mp}}{I_{sc}-I_{mp}}}\right); V \leq V_{mp} \\ I_{mp}\left(\frac{V_{mp}}{V}\right)\left(1-\left(\frac{V-V_{mp}}{V_{oc}-V_{mp}}\right)^{\phi}\right); V \geq V_{mp} \end{cases}, \quad (21)$$

where:

$$\phi = \left(\frac{I_{sc}}{I_{mp}}\right)\left(\frac{I_{sc}}{I_{sc}-I_{mp}}\right)\left(\frac{V_{oc}-V_{mp}}{V_{oc}}\right). \quad (22)$$

In the graph in Figure 2, these models are fitted to the experimental *I-V* curve for an RTC solar cell, taken from the well-known work by Easwarakhanthan et al. [83]. The 1-D/2-R equivalent circuit model is also fitted to these data, and it can be seen that the accuracy of the explicit models is quite high, as stated in [56,81]. The problem with using some of these models again lies in the need to solve the Lambert W-function, which requires some mathematical ability.

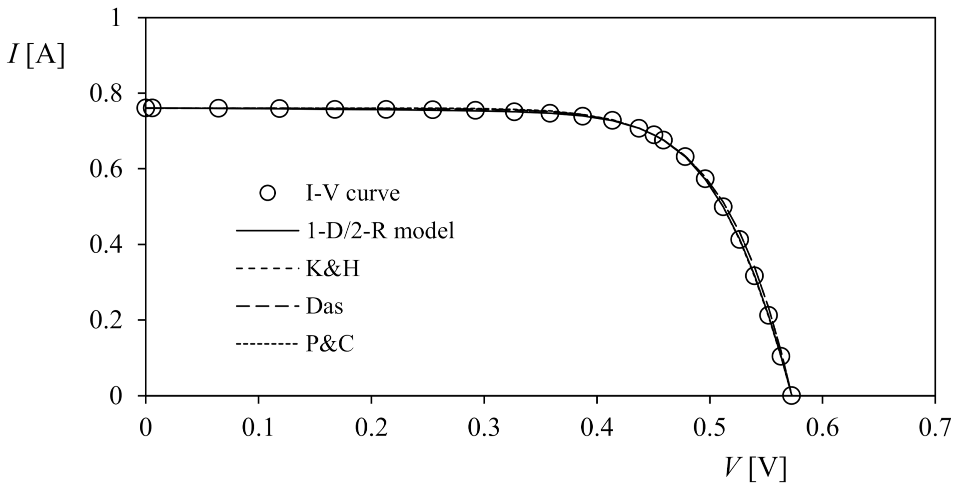

Figure 2. *I-V* curve of the RTC solar cell [83], with the results from the 1-D/2-R equivalent circuit model, and the explicit models of Kalmarkar and Haneefa, Das, and Pindado and Cubas.

2.3. The Lambert W-Function

From the methodologies described above, it is clear that in order to work with the equations of the implicit 1-D/2-R model and some of the explicit models, some knowledge of the Lambert W-function is required. The Lambert W-function, $W(z)$ (plotted in Figure 3), is defined as:

$$z = W(z)\exp(W(z)), \quad (23)$$

In the above equation, z is a complex number. If a real variable x is considered, the Lambert function is then defined within the range $[-1/\mathrm{e}, \infty]$. It should also be noted that this function gives a double value within the range $[-1/\mathrm{e}, 0]$. Two different branches, called the positive and negative branches, are normally defined for this function, as follows:

- $W_0(x)$, for $W(x) \geq -1$, and
- $W_{-1}(x)$, for $W(x) \leq -1$.

This function is a useful tool for solving equations that involve exponentials since if $X = Y\exp(Y)$, then $Y = W(X)$. However, as stated above, a certain level of expertise is required to solve these [84,85]. Barry et al. developed an interesting explicit approach, although this may not be sufficiently direct to obtain a solution [86].

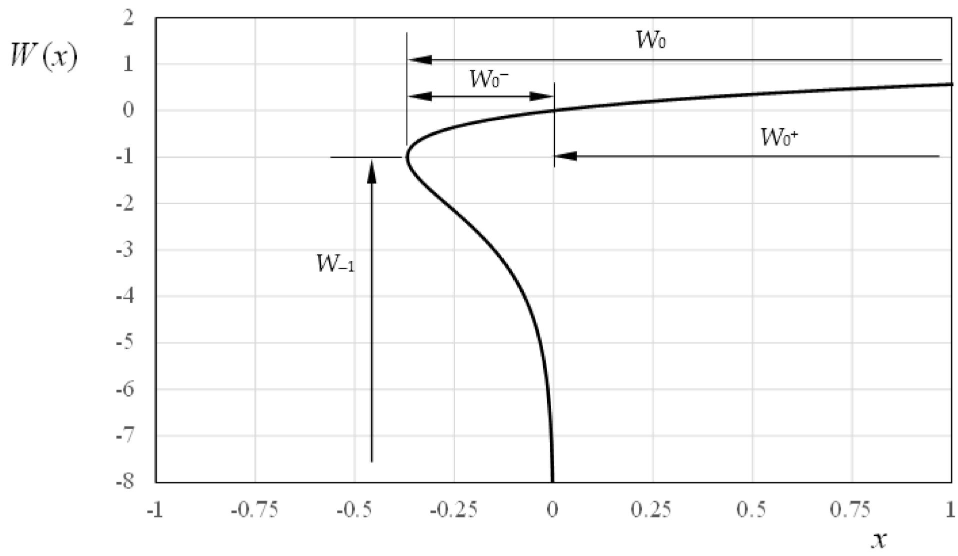

Figure 3. The Lambert W-function, with its two different branches.

3. Results

In this section, a method that facilitates the use of the 1-D/2-R equivalent circuit model is presented. It is organized into three sub-sections, as follows:

- Sub-Section 3.1 describes the problem of selecting a suitable value for the ideality factor, a, in order to obtain the values for the rest of the parameters.
- Very simple equations for the Lambert W-function, for use in solving the equations described in the section above, are included in Sub-Section 3.2.
- Finally, a case study in which our methodologies are applied to the modeling of spacecraft solar panels is included in Sub-Section 3.3.

3.1. On the Best Value for the Ideality Factor

In a paper published in the 2nd International Conference on Renewable Energy Research and Applications (ICRERA 2013), our research group demonstrated a hyperbolic relationship between the non-dimensional RMSE, ξ, of the 1-D/2-R equivalent circuit model fitted to the *I-V* curve of a solar cell, and the value of the ideality factor, a [87]. The non-dimensional (or normalized) RMSE is defined as:

$$\xi = \frac{\text{RMSE}}{I_{sc}} = \frac{1}{I_{sc}}\sqrt{\frac{1}{N}\sum_{i=1}^{N}\left(I - I_{ref}\right)^2}, \tag{24}$$

where N is the number of point of the *I-V* curve, I is the current obtained from modeling the corresponding solar cell/panel, and I_{ref} is the measured current associated with each one of those points. The aforementioned relationship between ξ and a is plotted in Figure 4. It can be seen that the curve has a hyperbolic shape, with a minimum value of the non-dimensional RMSE at a = 1.18. This hyperbolic shape was also confirmed in a recent work by Elkholy and Abou El-Ela [88].

The normalized RMSE can be used to compare the accuracy of different models applied to different photovoltaic technologies. However, it should also be taken into account that variations in temperature and irradiance could somehow affect the accuracy of the model's accuracy. In the present work, the current at the short circuit from the reference *I-V* curve has been selected as it was in previous works such as [57]. This way to normalize the RMSE has been used by other authors [89]. However, it was not the only one, as the average current value from the measured dataset that represents the *I-V* curve [88,90], or the difference between the current at two points [91], has also been proposed as current values to normalize the RMSE.

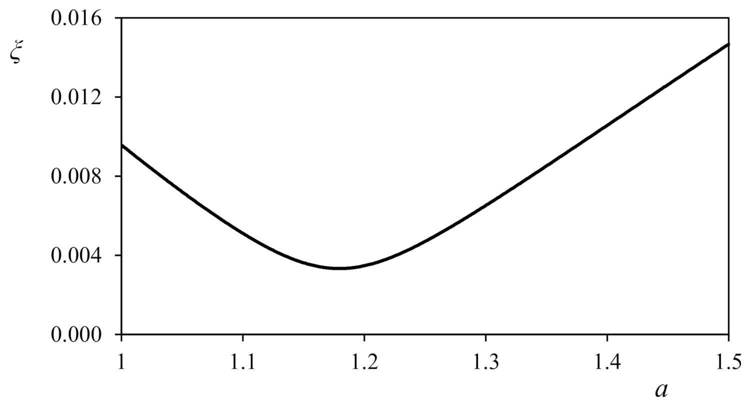

Figure 4. Non-dimensional RMSE, ξ, for a 1-D/2-R equivalent circuit model fitted to the *I-V* curve of an Emcore ZTJ solar cell (see Figure 1) versus the ideality factor, a.

The value of the ideality factor, a, was studied with the aim of providing future researchers with an accurate but much simpler fitting of the 1-D/2-R equivalent circuit model. To carry out this analysis, the *I-V* curves from four solar cells and three solar panels were selected from previous works [56,81], as shown in Table 1. The parameters extracted by fitting Equation (1) to these *I-V* curves using Matlab© are given in Table 2. These fits were used as a reference for the values calculated analytically since it could be reasonably assumed that they were the most accurate ones for the *I-V* curves. It should also be remarked that the equations for the 1-D/2-R equivalent circuit model resulting from these fits may not exactly meet the requirements for the short circuit, MPP, and open-circuit conditions, as they represent the best fits not only to the three characteristic points but to a large number of additional points.

Table 1. Solar cell/panel *I-V* curves used in the present work (where n is the number of series-connected cells for each of these photovoltaic devices; T is the temperature; and the characteristic points are I_{sc}, I_{mp}, V_{mp}, and V_{oc}).

Solar Cell/Panel	Technology	n	T [°C]	I_{sc} [A]	I_{mp} [A]	V_{mp} [V]	V_{oc} [V]
RTC France [1]	Si	1	33	0.7605	0.6894	0.4507	0.5727
TNJ Spectrolab [2]	GaInP2/GaAs/Ge	3	28	0.5259	0.4969	2.273	2.592
ZTJ Emcore [2]	InGaP/InGaAs/Ge	3	28	0.4634	0.4424	2.398	2.726
Azur Space 3G30C [3]	GaInP/GaAs/Ge	3	28	0.5270	0.5023	2.468	2.711
Photowatt PWP 201 [1]	Si	36	45	1.032	0.9255	12.493	16.778
Kyocera KC200GT-2 [2]	Si polycrystalline	54	25	8.182	7.605	26.90	32.92
Selex Galileo SPVS X5 [4]	GaInP/GaAs/Ge	15	20	0.5029	0.4783	12.406	13.603

[1] Taken from Easwarakhantan et al. [83]. [2] Graphically extracted from the manufacturer's datasheet. [3] Supplied by Azur Space. [4] Measured at CIEMAT (Spain).

Table 2. Parameters for the 1-D/2-E equivalent circuit models, numerically fitted to *I-V* curves based on data from RTC France, TNJ Spectrolab, ZTJ Emcore, and Azrur Space 3G30C solar cells, and Photowatt PWP 201, Kyocera KC200GT-2, and Selex Galileo SPVS X5 solar panels (where ξ is the non-dimensional RMSE for the fit).

Solar Cell/Panel	I_{pv} [A]	I_0 [A]	a	R_s [Ω]	R_{sh} [Ω]	ξ
RTC France	$7.617{\cdot}10^{-01}$	$2.746{\cdot}10^{-07}$	1.466	$3.697{\cdot}10^{-02}$	$4.421{\cdot}10^{+01}$	$8.49{\cdot}10^{-04}$
TNJ Spectrolab	$5.261{\cdot}10^{-01}$	$7.543{\cdot}10^{-15}$	1.045	$1.033{\cdot}10^{-01}$	$2.315{\cdot}10^{+02}$	$3.80{\cdot}10^{-03}$
ZTJ Emcore	$4.640{\cdot}10^{-01}$	$5.863{\cdot}10^{-14}$	1.180	$5.918{\cdot}10^{-02}$	$4.669{\cdot}10^{+02}$	$3.00{\cdot}10^{-03}$
Azur Space 3G30C	$5.274{\cdot}10^{-01}$	$8.522{\cdot}10^{-19}$	0.850	$8.580{\cdot}10^{-02}$	$2.202{\cdot}10^{+03}$	$1.57{\cdot}10^{-03}$
Photowatt PWP 201	$1.033{\cdot}10^{+00}$	$1.732{\cdot}10^{-06}$	1.282	$1.312{\cdot}10^{+00}$	$6.832{\cdot}10^{+02}$	$1.79{\cdot}10^{-03}$
Kyocera KC200GT-2	$8.179{\cdot}10^{+00}$	$2.693{\cdot}10^{-09}$	1.089	$2.280{\cdot}10^{-01}$	$1.449{\cdot}10^{+02}$	$3.53{\cdot}10^{-03}$
Selex Galileo SPVS X5	$4.994{\cdot}10^{-01}$	$6.165{\cdot}10^{-18}$	0.921	$1.885{\cdot}10^{-01}$	$1.422{\cdot}10^{+03}$	$6.50{\cdot}10^{-03}$

The 1-D/2-R equivalent circuit model was also analytically fitted to the aforementioned *I-V* curves. Using specific values for the ideality factor, a, and the characteristic points of the curve, I_{sc}, V_{mp}, I_{mp} and V_{oc}, the different parameters of the model were found using the following procedure:

- R_s was calculated using Equation (8) to (12);
- R_{sh} was calculated using Equation (5);
- I_{pv} was calculated using Equation (6);
- I_0 was calculated using Equation (7).

Once all the parameters were known, the *I-V* curve was found by obtaining the values of the current, I, for each value of the voltage, V, using Equation (13). The ideality factor was initially varied from a = 0.5 to a = 1.8 for each photovoltaic device (although this range was extended for some devices), and the non-dimensional RMSE, x, was calculated in each case. The results are plotted in Figure 5. Table 3 shows the values of the parameter a at which the minimum value of x is reached, with the rest of the parameters for the 1-D/2-R equivalent circuit.

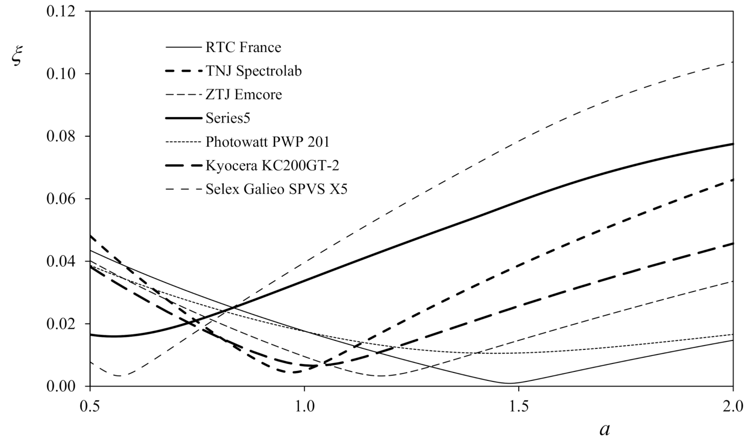

Figure 5. Non-dimensional RMSE, ξ, corresponding to the analytical approximations for extracting the 1-D/2-R equivalent circuit parameters in relation to the ideality factor, a, selected, for each one of the analyzed solar cells and panels.

Table 3. Parameters of the 1-D/2-R equivalent circuit models analytically fitted to *I-V* curves corresponding to data from RTC France, TNJ Spectrolab, ZTJ Emcore, and Azrur Space 3G30C solar cells, and Photowatt PWP 201, Kyocera KC200GT-2, and Selex Galileo SPVS X5 solar panels (where ξ is the non-dimensional RMSE for the fit).

Solar Cell/Panel	I_{pv} [A]	I_0 [A]	a	R_s [Ω]	R_{sh} [Ω]	ξ
RTC France	$7.610 \cdot 10^{-01}$	$3.200 \cdot 10^{-07}$	1.48	$3.621 \cdot 10^{-02}$	$5.195 \cdot 10^{+01}$	$9.33 \cdot 10^{-03}$
TNJ Spectrolab	$5.262 \cdot 10^{-01}$	$9.045 \cdot 10^{-16}$	0.98	$1.157 \cdot 10^{-01}$	$1.845 \cdot 10^{+02}$	$4.52 \cdot 10^{-03}$
ZTJ Emcore	$4.634 \cdot 10^{-01}$	$5.954 \cdot 10^{-14}$	1.18	$5.683 \cdot 10^{-02}$	$6.026 \cdot 10^{+02}$	$3.32 \cdot 10^{-03}$
Azur Space 3G30C	$5.275 \cdot 10^{-01}$	$5.012 \cdot 10^{-28}$	0.56	$1.322 \cdot 10^{-01}$	$1.554 \cdot 10^{+02}$	$1.60 \cdot 10^{-02}$
Photowatt PWP 201	$1.031 \cdot 10^{+00}$	$7.808 \cdot 10^{-06}$	1.44	$1.273 \cdot 10^{+00}$	$-1.121 \cdot 10^{+03}$	$1.06 \cdot 10^{-02}$
Kyocera KC200GT-2	$8.194 \cdot 10^{+00}$	$6.298 \cdot 10^{-10}$	1.02	$2.447 \cdot 10^{-01}$	$1.720 \cdot 10^{+02}$	$6.57 \cdot 10^{-03}$
Selex Galileo SPVS X5	$5.034 \cdot 10^{-01}$	$7.007 \cdot 10^{-29}$	0.56	$6.884 \cdot 10^{-01}$	$7.523 \cdot 10^{+02}$	$3.44 \cdot 10^{-03}$

Some important conclusions can be drawn based on these results, as follows:

- The analytical methodology suggested in the present work may give unacceptable results when the ideality factor exceeds a certain value, as complex numbers start to emerge in the calculations.
- One of the parameters obtained analytically for the best fit in terms of the non-dimensional RMSE has no physical meaning: this is the negative value of the resistance

of the shunt resistor shown in Table 3, which is obtained for the Photowatt PWP 201 solar panel.

- The best analytical fit gave remarkably low values of a in two cases: the Azur Space 3G30C solar cell, and the Selex Galileo SPVS X5 solar panel (composed of five Azur Space 3G28C series-connected cells), as their values were outside the range [1,1.5] suggested by Villalva et al. [74,75].

In order to compare both types of fit, the values of the ideality factor that gave the lowest values of x for the analytical fittings, $a_{bf\text{-}a}$, were plotted against the values obtained from the numerical fittings, $a_{bf\text{-}n}$, in Figure 6. It can be seen that the correlation between the fits is high, with the exception of only two devices: the Azur Space 3G30C solar cell, and the Selex Galileo SPVS X5 solar panel (which are both based on the same photovoltaic technology, as shown in Table 1). However, this correlation does not allow us to identify any rule that would suggest a reasonable value for the ideality factor. We, therefore, plotted the average values of the non-dimensional RMSE, ξ_{av}, obtained from the analytical fits versus the ideality factor, a. It can be seen from Figure 6 that the minimum value of ξ_{av} was obtained at a = 0.98. As a consequence, the value suggested for all devices is a = 1.

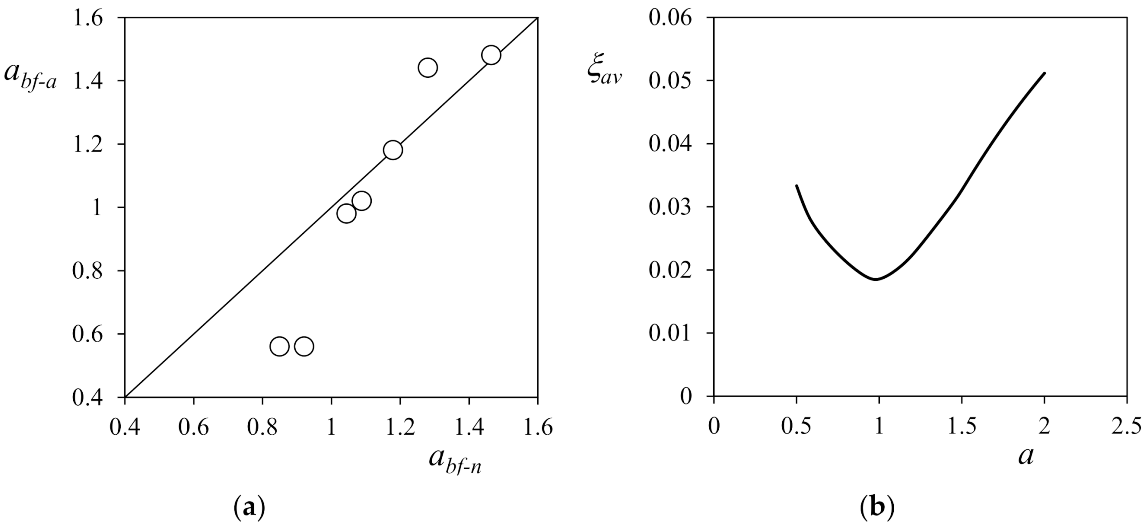

Figure 6. (**a**) Ideality factor corresponding to the best analytical fit to the 1-D/2-R equivalent circuit model, $a_{bf\text{-}a}$, for the studied *I-V* curves, versus ideality factors obtained from the numerical fittings, $a_{bf\text{-}n}$. The line corresponding to perfect correlation between both factors is shown as a reference. (**b**) Averaged non-dimensional RMSE for all analytical fittings, ξ_{av}, versus the ideality factor, a, used in the fits.

Figure 7 shows a comparison of the non-dimensional RMSE values obtained from the numerical fit, the analytical fit, and the analytical fit for a = 1 (see Table 4) for all of the photovoltaic devices. Although the differences may appear high, it should be taken into account that photovoltaic systems are normally designed to operate at the MPP, which is exactly reproduced by all of the analytical approximations for solving the parameter extraction of the 1-D/2-R equivalent circuit model. In addition, we reviewed the results from several works published over the last five years on parameter extraction for 1-D/2-R equivalent circuit models, based on the same experimental data from the RTC France solar cell and the Photowatt PWP 201 solar panel. The values obtained in these works for the non-dimensional RMSE for the fits were lower than the results from our method, with average values of $\xi = 1.20{\cdot}10^{-03}$ (RTC France solar cell) and $\xi = 4.03{\cdot}10^{-03}$ (Photowatt PWP 201 solar panel). Although these more accurate values were based on numerical rather than analytical procedures, it should be pointed out that numerical approaches do not always reach a more accurate solution [92].

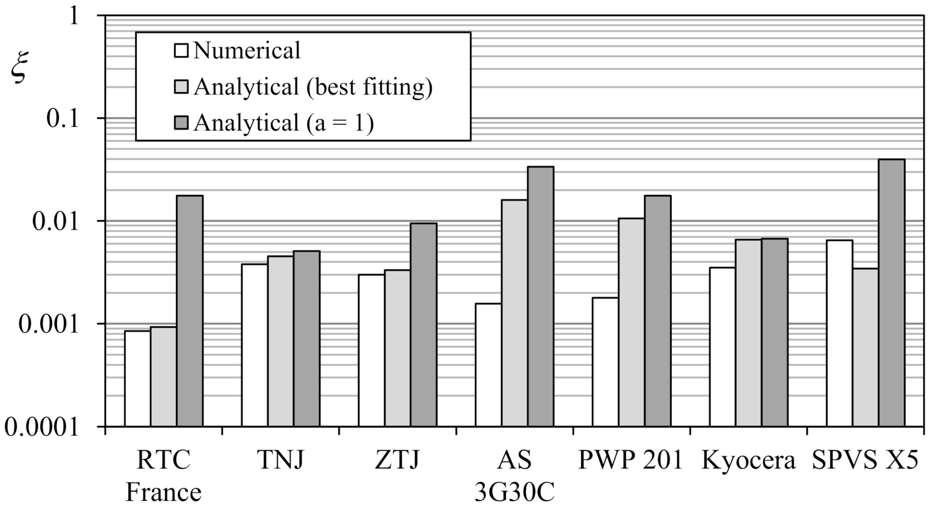

Figure 7. Values for the non-dimensional RMSE, *x*, obtained from a numerical fit of the 1-D/2-R equivalent circuit model to the studied *I-V* curves (see Table 2), an analytical fit (see Table 3), and an analytical fit with *a* = 1 (see Table 4).

Table 4. Analytically fitted parameters for 1-D/2-R equivalent circuit models, with *a* = 1, for *I-V* curves corresponding to RTC France, TNJ Spectrolab, ZTJ Emcore, and Azrur Space 3G30C solar cells, and Photowatt PWP 201, Kyocera KC200GT-2, and Selex Galileo SPVS X5 solar panels (where ξ is the non-dimensional RMSE for the fit).

Solar Cell/Panel	I_{pv} [A]	I_0 [A]	a	R_s [Ω]	R_{sh} [Ω]	ξ
RTC France	$7.638 \cdot 10^{-01}$	$2.721 \cdot 10^{-10}$	1	$6.912 \cdot 10^{-02}$	$1.615 \cdot 10^{+01}$	$1.77 \cdot 10^{-02}$
TNJ Spectrolab	$5.262 \cdot 10^{-01}$	$1.786 \cdot 10^{-15}$	1	$1.078 \cdot 10^{-01}$	$1.895 \cdot 10^{+02}$	$5.08 \cdot 10^{-03}$
ZTJ Emcore	$4.636 \cdot 10^{-01}$	$2.835 \cdot 10^{-16}$	1	$1.348 \cdot 10^{-01}$	$3.723 \cdot 10^{+02}$	$9.51 \cdot 10^{-03}$
Azur Space 3G30C	$5.269 \cdot 10^{-01}$	$3.881 \cdot 10^{-16}$	1	$-6.068 \cdot 10^{-02}$	$2.643 \cdot 10^{+02}$	$3.38 \cdot 10^{-02}$
Photowatt PWP 201	$1.036 \cdot 10^{+00}$	$4.163 \cdot 10^{-08}$	1	$1.982 \cdot 10^{+00}$	$5.430 \cdot 10^{+02}$	$1.76 \cdot 10^{-02}$
Kyocera KC200GT-2	$8.195 \cdot 10^{+00}$	$3.950 \cdot 10^{-10}$	1	$2.522 \cdot 10^{-01}$	$1.638 \cdot 10^{+02}$	$6.71 \cdot 10^{-03}$
Selex Galileo SPVS X5	$5.028 \cdot 10^{-01}$	$1.261 \cdot 10^{-16}$	1	$-3.091 \cdot 10^{-01}$	$1.185 \cdot 10^{+03}$	$3.96 \cdot 10^{-02}$

3.2. Lambert W-Function Simplified Equations for Solar Cell/Panel Modeling

A thorough review of the available literature from between 2000 and 2020 was carried out to find relevant data on photovoltaic devices, including the five parameters of the 1-D/2-R equivalent circuit model (I_{pv}, I_0, a, R_s, and R_{sh}), the characteristic points of the *I-V* curve (I_{sc}, V_{mp}, I_{mp}, and V_{oc}), the temperature of the cells, T, which is related to the performance curve, and the number of series-corrected cells, n. Information was found for 90 photovoltaic devices, most of which were solar panels.

The positive branch of the Lambert W-function needs to be solved for in Equation (13), and must be evaluated at certain points x for a given value of the output voltage, V (within the range [0, V_{oc}]):

$$x = f\left(I_{pv}, I_0, a, R_s, R_{sh}, n, T, V\right). \tag{25}$$

After post-processing the data from the 90 solar cells/panels, it was clear that Equation (13) refers to the right-side section of the Lambert's W-function positive branch, W_0^+. The following expressions were proposed:

$$W_0^+(x) = x \exp\left(0.71116x^2 - 0.98639x\right),\ x \in \left[2 \cdot 10^{-16}, 2 \cdot 10^{-1}\right], \tag{26}$$

$$W_0^+(x) = -1.6579 + 0.1396\left(2.9179 \cdot 10^5 - (x - 22.8345)^4\right)^{0.25},\ x \in [0.2, 1.2], \tag{27}$$

$$W_0^+(x) = -1.2216 + 3.4724 \cdot 10^{-2}\left(1.7091 \cdot 10^8 - (x - 114.146)^4\right)^{0.25}, \ x \in [1.2, 10]. \quad (28)$$

The error for these equations was below 0.15% (Equation (26)), 0.16% (Equation (27)), and 0.08% (Equation (28)). For larger values of x, we recommend using the approximation proposed by Barry et al. [86] (see Appendix A). In Figure 8, the positive branch of Lambert's W-function, W_0^+, calculated at the points x (Equation (25)) corresponding to the data for the solar cells/panels, evaluated at V = 0 and V = V_{oc}, is shown together with Equation (26) to (28). Depending on the magnitude of x (that is, depending on how closely it approaches 0^+), W_0^+ can be reasonably estimated as:

$$W_0^+ = x - 0.98639x^2 + 1.1976x^3 \approx x - 0.98639x^2 \approx x, \quad (29)$$

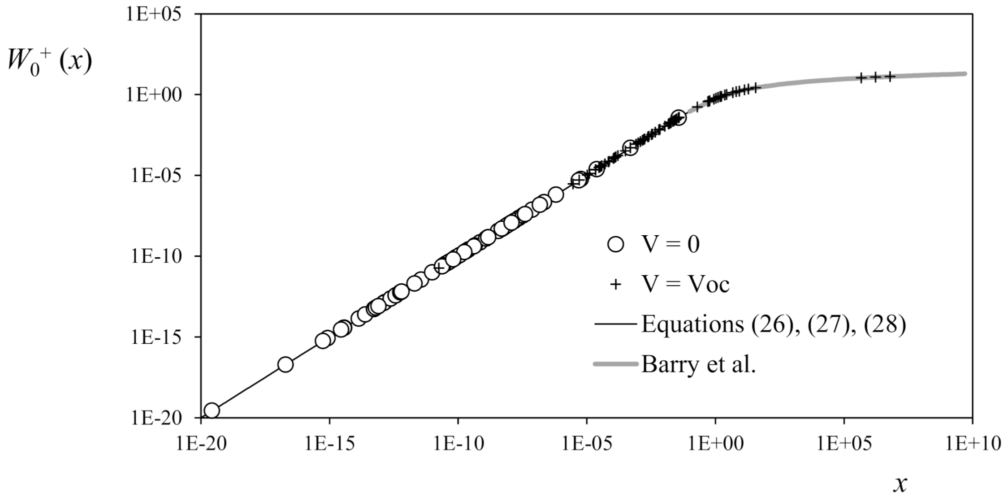

Figure 8. Positive branch of Lambert's W-function (right-side), W_0^+, calculated at V = 0 and V = V_{oc} for points x (Equation (25)) corresponding to the 1-D/2-R equivalent circuit model, based on the data for the solar cells/panels. Our approximation for W_0^+ (Equation (26) to (28)) is also shown.

The negative branch of the Lambert W-function, W_{-1}, needs to be calculated at:

$$x = f\left(I_{pv}, I_0, a, R_s, R_{sh}, n, T, V\right) \quad (30)$$

when estimating the series resistance, R_s, for the 1-D/2-R equivalent circuit model (Equation (8) to (12)). Since the above equation for the different solar cells/panels from the database gives values of x within the range $[-2.77 \cdot 10^{-3}, -10^{-35}]$, two expressions were defined:

$$W_{-1}(x) = 9.7117 \cdot 10^{-5} \ln(-x)^3 + 6.8669 \cdot 10^{-3} \ln(-x)^2 + 1.2 \ln(-x) - 1.1102, \\ x \in \left[-10^{-2}, -5 \cdot 10^{-13}\right] \quad (31)$$

$$W_{-1}(x) = 1.6705 \cdot 10^{-6} \ln(-x)^3 + 4.4514 \cdot 10^{-4} \ln(-x)^2 + 1.0511 \ln(-x) - 2.3364, \\ x \in \left[-5 \cdot 10^{-13}, -10^{-40}\right] . \quad (32)$$

The error for these equations was below 0.42% (Equation (31)) and 0.02% (Equation (32)) (see Figure 9). Equation (32) can be applied for values of up to $x = -10^{-50}$, with errors of below 0.07%.

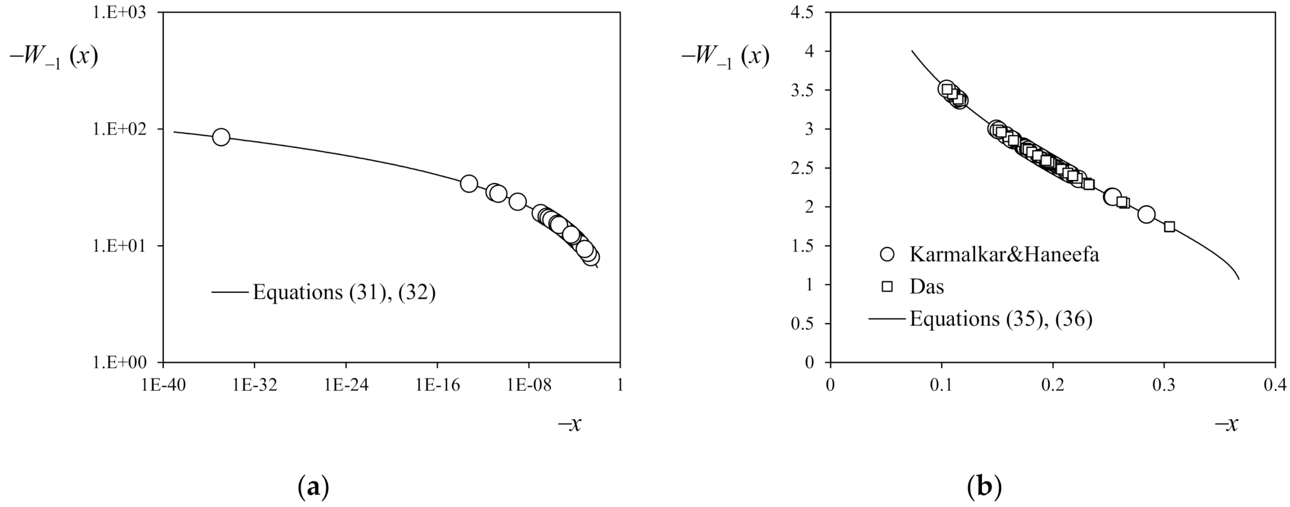

Figure 9. (**a**) Negative branch of Lambert's W-function, W_{-1}, calculated for points x (Equation (30)) corresponding to the series resistance, R_s, of the 1-D/2-R equivalent circuit model, based on data for solar cells/panels. Our approximate expression for W_{-1} (Equations (31) and (32)) is also shown. (**b**) Negative branch of Lambert's W-function, W_{-1}, calculated for points x (Equation (33)) corresponding to the explicit models proposed by Kalmarkar and Haneefa and Das, based on data for solar cells/panels. Our approximate expression for W_{-1} (Equations (35) and (36)) is also shown.

Finally, if the explicit models proposed by Kalmarkar and Haneefa, and Das are used, W_{-1} needs to be calculated at points x defined by the characteristic points of the *I-V* curve (I_{sc}, V_{mp}, I_{mp}, and V_{oc} (see Equations (16) and (19)):

$$x = f\left(I_{sc}, I_{mp}, V_{oc}, V_{mp}\right) \tag{33}$$

as shown in Figure 9. Based on the post-processed data for the 90 solar cells/panels, the values of x calculated using these explicit methods were within the range [−0.304, −0.1]. The following equation for W_{-1} was initially suggested, which was characterized by an error of less than 1.6%22 within this range:

$$W_{-1}(x) = 248.42x^4 + 134.24x^3 + 4.4258x^2 - 14.629x - 4.9631 \tag{34}$$

In order to extend both the range of validity and the accuracy of the above equation, a splitting into two sub-branches at the point where the curvature of the function changes its sign ($x = -0.27$), the following equations were suggested:

$$W_{-1}(x) = -1 - \sqrt{42.949x^2 + 37.694x + 8.0542},\ x \in [-0.36785, -0.27] \tag{35}$$

$$W_{-1}(x) = 0.14279\ln(-x)^3 + 1.04416\ln(-x)^2 + 3.92\ln(-x) + 1.65795,\quad x \in [-0.27, -0.0732] \tag{36}$$

The error for the above equations was below 0.23% (Equation (35)) and 0.02% (Equation (36)) (see Figure 9). It should also be emphasized that caution needs to be used with regard to Equation (35), as it gives complex solutions when $x \to -1/e^+$ (that is, when $x \in [-1/e, -0.36785]$).

3.3. Case Study: The Solar Panels of the UPMSat-1

The general characteristics from the *I-V* curves for the UPM-5 and UPM-6 solar panels for UPMSat-1 (see Figure 10) are shown in Tables 1, 2 and 5 (Appendix B). These panels are based on two different technologies: Si (UPM-5) and Ga-As (UPM-6). In the latter, the number of series-connected cells n was 32; however, since they were based on double-junction technology, this number must be multiplied by two, unlike in the

1-D/2-R equivalent circuit model (the Selex Galileo SPVS X5, formed from five Azur Space triple-junction technology series-connected solar cells, where n = 15, as shown in Table 1).

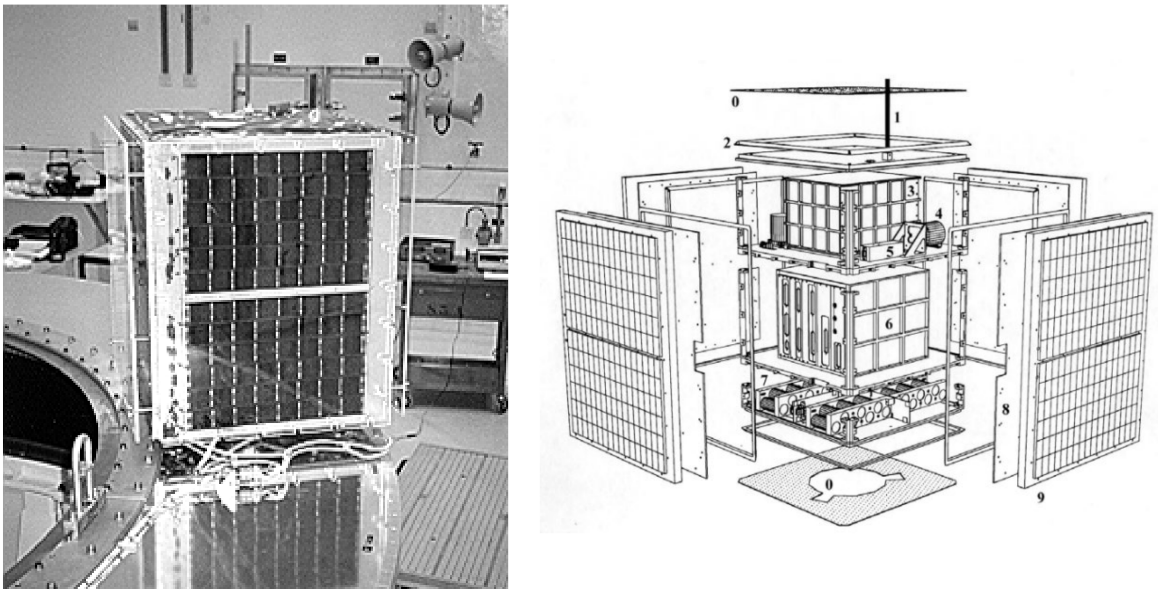

(**a**) (**b**)

Figure 10. The UPMSat-1 satellite; launched in 1995, this was the tenth university-developed space mission in history [93]. (**a**) Satellite during the integration in the Ariane IV-40 launcher (V75 flight). (**b**) Exploded view drawing.

Table 5. Characteristics of the measured *I-V* curves corresponding to the UPM-5 and UPM-6 solar panels of UPMSat-1 (see Figure 10).

Solar Panel	Technology	n	T [°C]	I_{sc} [A]	I_{mp} [A]	V_{mp} [V]	V_{oc} [V]
UPM-5	Si	51	25	1.431	1.329	25.139	30.513
UPM-6	Ga-As	64	25	1.423	1.318	25.806	31.351

The *I-V* curves for the UPM-5 and UPM-6 solar panels are plotted in Figures 11 and 12, respectively, with several other curves corresponding to:

- The best fit of the 1-D/2-R equivalent circuit model (see Table 6);
- The analytical fit for a = 1 (Equations (5–12)), and our approximations to the Lambert W-function (Equations (26)–(28),(31,32));
- The explicit models proposed by Kalmarkar and Haneefa, Das (Equations (14)–(20), (35,36)), and Pindado and Cubas (Equations (21) and (22)), see Table 7.

Table 6. Parameters for the 1-D/2-R equivalent circuit model (where Num. represents the numerical best fit, and An. represents the analytical fit with a = 1) for the UPM-5 and UPM-6 solar panels of the UPMSat-1 satellite. ξ is the non-dimensional RMSE for the experimental data.

Solar Panel	Fitting	I_{pv} [A]	I_0 [A]	a	R_s [Ω]	R_{sh} [Ω]	ξ
UPM-5	Num.	1.4314	$1.0495{\cdot}10^{-09}$	1.105	1.0368	$4.3761{\cdot}10^{+03}$	$1.80{\cdot}10^{-03}$
	An.	1.4323	$1.0855{\cdot}10^{-10}$	1	1.2045	$1.3023{\cdot}10^{+03}$	$5.63{\cdot}10^{-03}$
UPM-6	Num.	1.4295	$1.0285{\cdot}10^{-09}$	0.902	0.8483	$9.9115{\cdot}10^{+02}$	$9.50{\cdot}10^{-03}$
	An.	1.4238	$7.3448{\cdot}10^{-09}$	1	0.7207	$1.3524{\cdot}10^{+03}$	$1.70{\cdot}10^{-02}$

Table 7. Parameters for the explicit models proposed by Kalmarkar and Haneefa, Das and Pindado and Cubas, for the UPM-5 and UPM-6 solar panels of the UPMSat-1 satellite. ξ is the non-dimensional RMSE for the experimental data.

Model	Parameters; ξ	UPM-5	UPM-6
Kalmarkar and Haneefa	γ	$9.942{\cdot}10^{-01}$	$9.912{\cdot}10^{-01}$
	m	$1.401{\cdot}10^{-01}$	$1.392{\cdot}10^{-01}$
	ξ	$3.35{\cdot}10^{-02}$	$3.71{\cdot}10^{-02}$
Das	k	$1.401{\cdot}10^{-01}$	$1.393{\cdot}10^{-01}$
	h	$6.526{\cdot}10^{-03}$	$9.568{\cdot}10^{-03}$
	ξ	$3.33{\cdot}10^{-02}$	$3.69{\cdot}10^{-02}$
Pindado and Cubas	ϕ	2.6605	2.5879
	ξ	$2.04{\cdot}10^{-02}$	$2.12{\cdot}10^{-02}$

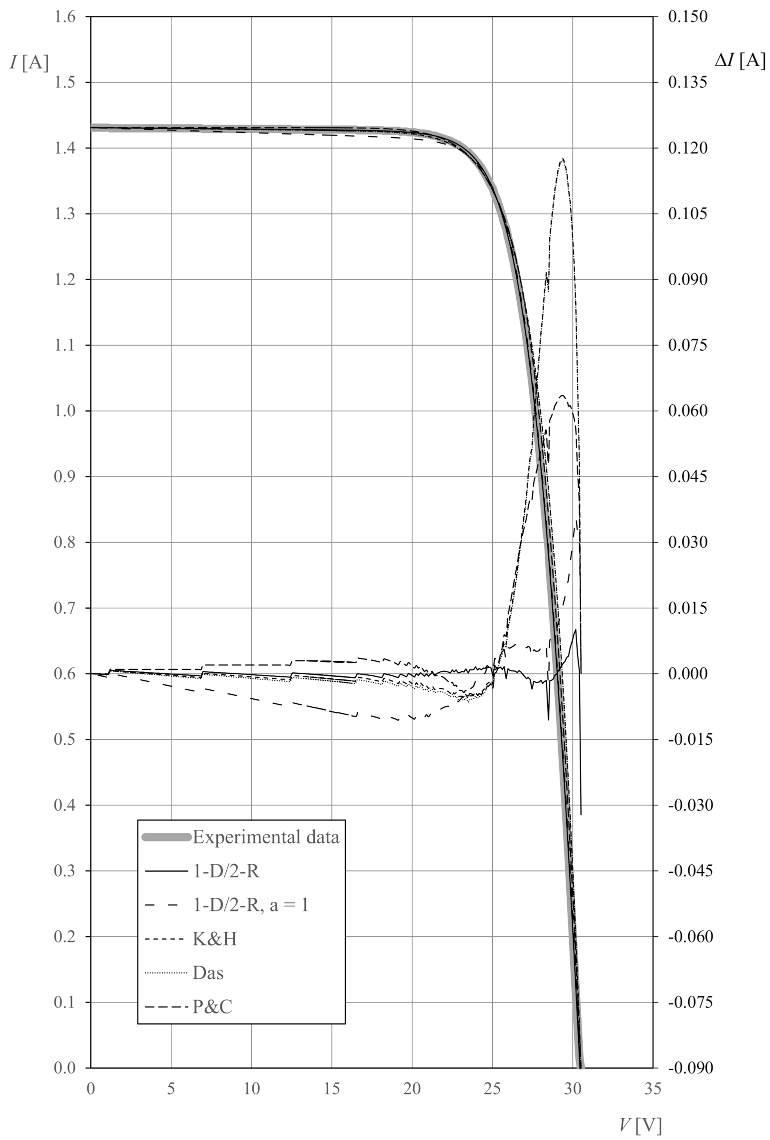

Figure 11. *I-V* experimental curve (left axis) for the UPM-5 solar panel. Curves for the 1-D/2-R equivalent circuit model (obtained using two procedures: best fit to the parameters obtained numerically and analytical extraction) and the explicit methods proposed by Kalmarkar and Haneefa, Das and Pindado and Cubas are shown. The differences in the current compared to the experimental data are indicated on the right axis.

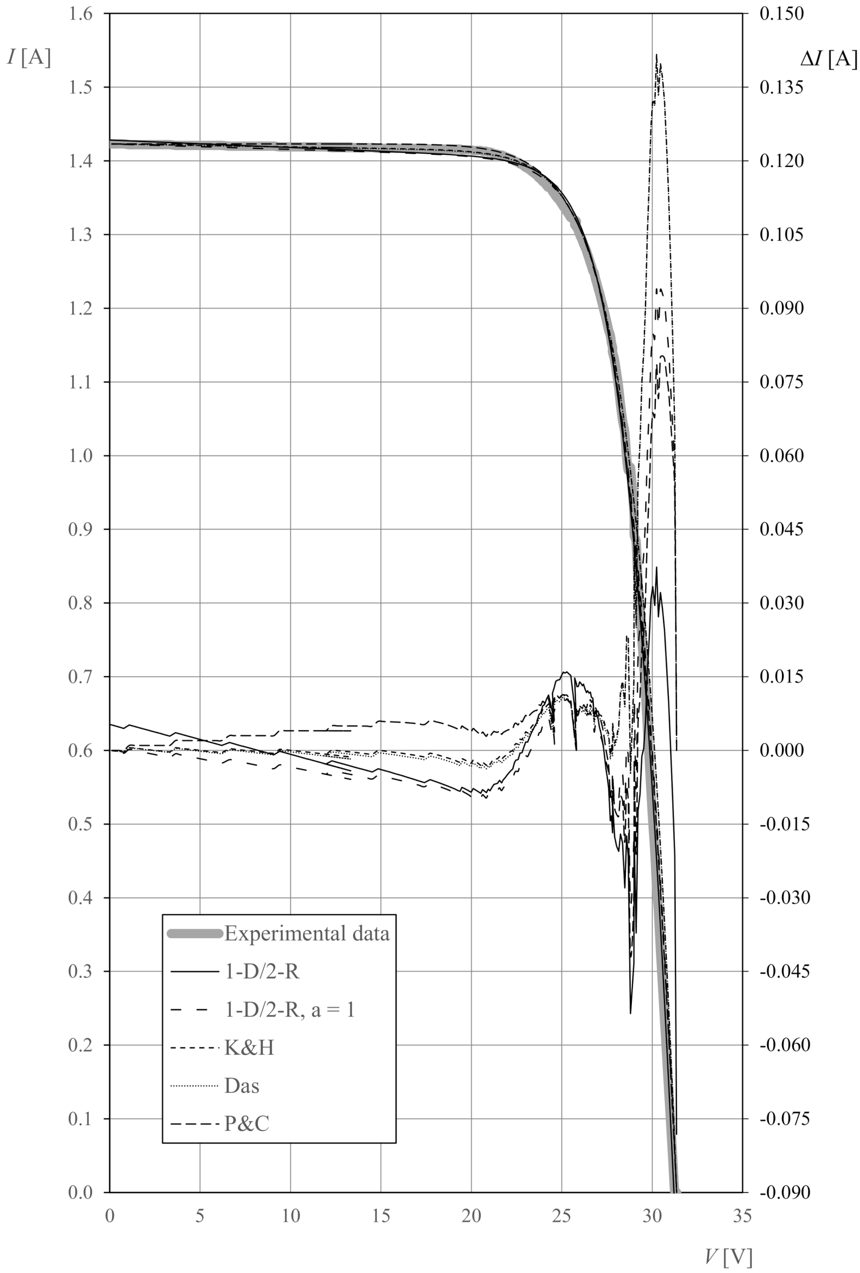

Figure 12. *I-V* experimental curve (left axis) for the UPM-6 solar panel. Curves for the 1-D/2-R equivalent circuit model (obtained using two procedures: best fit to the parameters obtained numerically and analytical extraction) and the explicit methods of Kalmarkar and Haneefa, Das and Pindado and Cubas are shown. The differences in the current compared to the experimental data are indicated on the right axis.

The differences in the current for these models with regard to the experimental *I-V* curves are plotted in Figures 11 and 12.

The differences were relatively small, with the maximum always located in a reasonably small range between the MPP and the open voltage point. The values of the non-dimensional RMSE, ξ, for the fits are plotted in Figure 13. The results show reasonably good agreement with the mathematical approaches proposed in the present work.

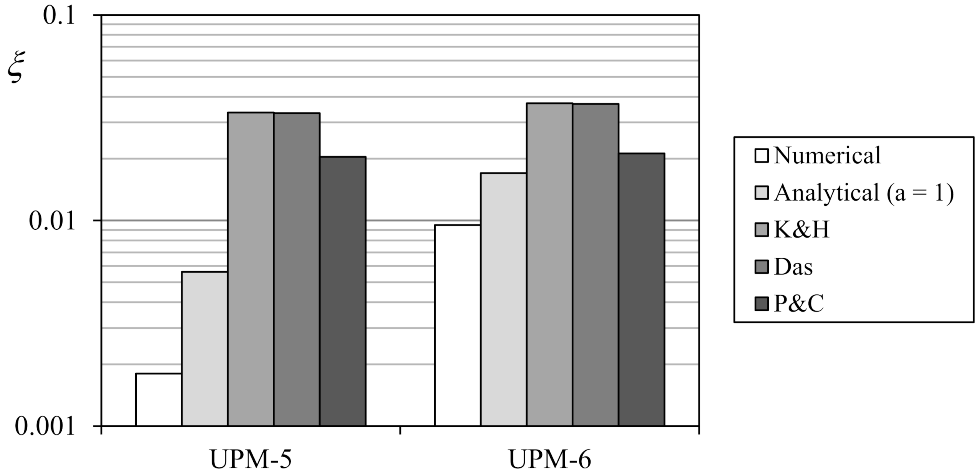

Figure 13. Non-dimensional RMSE, ξ, for the numerical fit of the 1-D/2-R equivalent circuit model, and the analytical fit with the proposed method, for the UPM-5 and UPM-6 solar panels of UPMSat-1. Values derived from the explicit methods studied here are also shown.

4. Conclusions

In this study, we have reviewed analytical approaches for extracting the five parameters of the 1-D/2-R equivalent circuit model from the characteristic points of the *I-V* curve (short circuit, MPP, and open circuit points). Five different problems were identified, as follows:

- An initial estimation of the ideality factor, a, is required.
- The equation for the value of the resistance of the series-connected resistor, Rs, is an implicit expression, meaning that either an iterative process or the Lambert W-function is required.
- When all the parameters for the 1-D/2-R equivalent circuit model have been extracted, an implicit equation must be solved (or the Lambert W-function must be used) to derive the value of the output current for a given output voltage.
- The use of the Lambert W-function requires some numerical and calculation resources and skills.
- The use of explicit models rather than the 1-D/2-R equivalent circuit model, in order to avoid the problems described above, may not be possible, as some of them require the Lambert W-function to derive their parameters, based on the characteristic points of the *I-V* curve.

I-V curves from seven different solar cells/panels were used to test our proposed approach. *I-V* curves from two of the solar panels of the UPMSat-1 spacecraft were also analyzed as a case study.

The most important conclusions of this work are as follows:

- A value of a = 1 for the 1-D/2-R equivalent circuit model was shown to be reasonable for most photovoltaic technologies.
- The analytical procedure for extracting the parameters for the 1-D/2-R equivalent circuit model may give values for the resistance of one resistor (or even both) that are negative. However, this does not affect the results (i.e., the modeled performance of the photovoltaic device).
- The Lambert W-function can be simplified for use in modeling the performance of photovoltaic devices. Accurate simplified versions of the Lambert W-function are proposed here for three cases, depending on the specific need: (i) calculation of Rs; (ii) calculation of the output current using the equation for the 1-D/2-R equivalent circuit; or (iii) calculation of the parameters for certain explicit models.
- Explicit models are also accurate alternatives to the 1-D/2-R equivalent circuit model.

Our approach was carefully verified in a case study in which the fits of the1-D/2-R equivalent circuit model and the explicit methods to the measured data (*I-V* curve) for two solar panels from the UPMSat-1 satellite were compared with the results of the proposed method.

Finally, it should be highlighted that the results from this work open up new possibilities for coupled calculations, both for the performance of photovoltaic systems and in other disciplines such as thermodynamics and power distribution in grids. The simple but accurate solutions to the 1-D/2-R equivalent circuit model and the explicit methods described here can easily be implemented in software packages such as ESATAN©.

Author Contributions: Project administration, S.P., J.C., E.R.-M.; methodology, S.P.; conceptualization, S.P.; formal analysis, S.P.; supervision S.P., J.C., E.R.-M.; investigation, J.M.Á., D.A.-C., J.C.-E., M.S.-P., R.J.-P., A.G.-E.; software, J.M.Á., D.A.-C., J.C.-E., M.S.-P., R.J.-P., A.G.-E.; validation, visualization, J.M.Á., D.A.-C., J.C.-E., M.S.-P., R.J.-P., A.G.-E.; writing—original draft, J.M.Á., D.A.-C., E.R.-M., J.C.-E., M.S.-P., R.J.-P., A.G.-E.; writing—review and editing, S.P. All authors have read and agreed to the published version of the manuscript.

Funding: This research received no external funding.

Institutional Review Board Statement: Not applicable.

Informed Consent Statement: Not applicable.

Data Availability Statement: Not applicable.

Acknowledgments: This work was carried out within the framework of the Educational Innovation Project PIE IE1920.1402 'PIRAMIDE: *Proyectos de Investigación Realizados por Alumnos de Máster/Grado para la Innovación y el Desarrollo Espacial*'. This Academic Innovation Project (AIP) was funded by *Universidad Politécnica de Madrid* (UPM) in the 2019/2020 call '*Ayudas a la innovación educativa y a la mejora en la calidad de la enseñanza*'. The authors are indebted to Ángel Sanz-Andrés for his support with regard to the research program on the performance of solar panels at *Instituto Universitario de Microgravedad "Ignacio Da Riva"* (IDR/UPM), *Universidad Politécnica de Madrid* (UPM). The authors are grateful to the reviewers for their kind help in improving the present paper.

Conflicts of Interest: The authors declare no conflict of interest.

Appendix A. Approximation to the Right-Side of the Lambert W-Function Positive Branch by Larry et al. (2000) (see References)

$$W_0^+(x) = 1.4586887 \ln\left(\frac{1.2x}{\ln(2.4x/\ln(1+2.4x))}\right) - 0.4586887 \ln\left(\frac{2x}{\ln(1+2x)}\right). \tag{A1}$$

Appendix B. *I-V* Curves of the UPMSat-1 Solar Panels.

Table 1. *I-V* curve of the UPM-5 solar panel of the UPMSat-1.

V [V]	*I* [A]	*V* [V]	*I* [A]	*V* [V]	*I* [A]	*V* [V]	*I* [A]	*V* [V]	*I* [A]	*V* [V]	*I* [A]
−0.950	1.431	5.189	1.430	10.813	1.429	16.204	1.428	21.510	1.418	26.428	1.213
−0.801	1.431	5.330	1.430	10.944	1.429	13.338	1.428	21.632	1.417	26.545	1.198
−0.660	1.431	5.471	1.430	11.077	1.429	16.459	1.428	21.758	1.416	26.657	1.182
−0.510	1.431	5.613	1.430	11.217	1.429	16.589	1.427	21.879	1.415	26.775	1.165
−0.370	1.431	5.744	1.430	11.348	1.429	16.723	1.427	22.001	1.414	26.887	1.148
−0.221	1.431	5.888	1.430	11.480	1.429	16.848	1.427	22.128	1.413	27.006	1.129
−0.079	1.431	6.026	1.430	11.614	1.429	16.980	1.427	22.248	1.412	27.118	1.110
0.067	1.431	6.167	1.430	11.745	1.429	17.101	1.427	22.372	1.411	27.226	1.090
0.210	1.431	6.309	1.430	11.885	1.429	17.234	1.427	22.493	1.409	27.343	1.068
0.360	1.431	6.440	1.430	12.019	1.429	17.388	1.427	22.617	1.408	27.453	1.048

Table 1. *Cont.*

V [V]	*I* [A]	*V* [V]	*I* [A]	*V* [V]	*I* [A]	*V* [V]	*I* [A]	*V* [V]	*I* [A]	*V* [V]	*I* [A]
0.600	1.431	6.580	1.430	12.149	1.429	17.489	1.427	22.741	1.406	27.572	1.021
0.660	1.431	6.727	1.430	12.282	1.429	17.621	1.427	22.861	1.405	27.681	0.997
0.782	1.431	6.863	1.430	12.413	1.429	17.744	1.427	22.987	1.403	27.789	0.972
0.924	1.431	6.983	1.429	12.545	1.428	17.999	1.427	23.099	1.401	27.908	0.943
1.071	1.431	7.136	1.429	12.678	1.428	18.122	1.427	23.221	1.399	28.013	0.916
1.214	1.430	7.277	1.429	12.810	1.428	18.253	1.426	23.343	1.396	28.122	0.888
1.364	1.430	7.407	1.429	12.942	1.428	18.278	1.426	23.485	1.394	28.230	0.858
1.503	1.430	7.546	1.429	13.075	1.428	18.510	1.426	23.588	1.391	28.345	0.825
1.643	1.430	7.689	1.429	13.206	1.428	18.635	1.426	23.712	1.388	28.483	0.793
1.786	1.430	7.822	1.429	13.336	1.428	18.756	1.426	23.827	1.385	28.558	0.761
1.936	1.430	7.963	1.429	13.470	1.428	18.889	1.426	23.948	1.381	28.665	0.727
2.076	1.430	8.094	1.429	13.601	1.428	19.011	1.426	24.071	1.378	28.780	0.689
2.216	1.430	8.235	1.429	13.734	1.428	19.138	1.426	24.183	1.374	28.884	0.653
2.367	1.430	8.374	1.429	13.884	1.428	19.267	1.425	24.305	1.370	28.992	0.615
2.508	1.430	8.507	1.429	13.997	1.428	19.390	1.425	24.427	1.365	29.096	0.577
2.648	1.430	8.648	1.429	14.129	1.428	19.514	1.425	24.550	1.360	29.200	0.538
2.709	1.430	8.780	1.429	14.262	1.428	19.648	1.425	24.671	1.354	29.314	0.494
2.930	1.430	8.923	1.429	14.392	1.428	19.769	1.424	24.784	1.349	29.420	0.452
3.068	1.430	9.053	1.429	14.515	1.428	19.892	1.424	24.905	1.343	29.524	0.410
3.219	1.430	9.194	1.429	14.649	1.428	20.016	1.424	25.027	1.338	29.629	0.366
3.359	1.430	9.325	1.429	14.780	1.428	20.146	1.424	25.139	1.329	29.738	0.320
3.500	1.430	9.456	1.429	14.911	1.428	20.263	1.423	25.261	1.322	29.847	0.271
3.642	1.430	9.598	1.429	15.042	1.428	20.395	1.423	25.377	1.314	29.960	0.220
4.064	1.430	9.730	1.429	15.168	1.428	20.518	1.422	25.496	1.305	30.074	0.167
4.204	1.430	9.870	1.429	16.297	1.428	20.639	1.422	25.617	1.296	30.189	0.113
4.347	1.430	10.003	1.429	15.430	1.428	20.762	1.422	25.729	1.286	30.299	0.067
4.485	1.430	10.136	1.429	15.561	1.428	20.896	1.421	25.848	1.278	30.409	0.018
4.628	1.430	10.275	1.429	15.666	1.428	21.018	1.421	25.961	1.265	30.513	0.000
4.767	1.430	10.407	1.429	15.815	1.428	21.140	1.420	26.082	1.253		
4.909	1.430	10.540	1.429	15.949	1.428	21.265	1.419	26.193	1.241		
5.047	1.430	10.661	1.429	16.082	1.428	21.388	1.419	26.314	1.227		

Table 2. *I-V* curve of the UPM-6 solar panel of the UPMSat-1.

V [V]	*I* [A]	*V* [V]	*I* [A]	*V* [V]	*I* [A]	*V* [V]	*I* [A]	*V* [V]	*I* [A]	*V* [V]	*I* [A]
−0.638	1.423	9.402	1.419	19.166	1.416	22.469	1.399	25.814	1.310	28.142	1.093
−0.518	1.423	9.722	1.419	19.269	1.416	22.593	1.398	25.844	1.309	28.249	1.069
−0.198	1.423	10.042	1.419	19.373	1.416	22.687	1.396	25.917	1.305	28.367	1.047
0.122	1.423	10.362	1.419	19.476	1.415	22.801	1.395	25.990	1.300	28.485	1.031
0.442	1.423	10.882	1.419	19.560	1.415	22.905	1.393	26.063	1.296	28.581	0.999
0.782	1.423	11.002	1.419	19.684	1.415	23.009	1.391	26.136	1.292	28.680	0.980
1.082	1.422	13.322	1.419	19.788	1.415	23.113	1.390	26.209	1.287	28.795	0.984
1.402	1.422	11.842	1.419	19.892	1.415	23.217	1.388	26.282	1.283	28.990	0.923
1.722	1.422	11.962	1.419	19.986	1.415	23.320	1.386	26.365	1.278	29.007	0.892
2.042	1.422	12.282	1.418	20.100	1.414	23.424	1.384	26.428	1.273	29.112	0.883
2.362	1.422	12.602	1.418	20.204	1.414	23.528	1.382	26.500	1.268	29.216	0.828
2.882	1.422	12.922	1.418	20.308	1.414	23.632	1.380	26.573	1.262	29.321	0.793
3.002	1.422	13.242	1.418	20.411	1.414	23.736	1.377	26.646	1.257	29.424	0.753
3.322	1.422	13.682	1.418	20.515	1.414	23.840	1.375	26.718	1.251	29.527	0.718
3.642	1.421	13.882	1.418	20.619	1.413	23.944	1.372	26.792	1.248	29.630	0.678
3.882	1.421	14.202	1.418	20.723	1.413	24.048	1.370	26.865	1.240	29.732	0.632

Table 2. *Cont.*

V [V]	*I* [A]	*V* [V]	*I* [A]	*V* [V]	*I* [A]	*V* [V]	*I* [A]	*V* [V]	*I* [A]	*V* [V]	*I* [A]
4.282	1.421	14.522	1.418	20.827	1.413	24.152	1.367	26.938	1.234	29.834	0.589
4.602	1.421	14.842	1.417	20.931	1.412	24.265	1.364	27.011	1.227	29.935	0.543
4.922	1.421	15.162	1.417	21.035	1.412	24.590	1.362	27.084	1.221	30.035	0.502
5.242	1.421	15.482	1.417	21.139	1.411	24.483	1.359	27.157	1.214	30.138	0.465
5.562	1.421	15.802	1.417	21.243	1.410	24.567	1.356	27.230	1.207	30.239	0.416
5.882	1.421	16.122	1.417	21.248	1.410	24.671	1.352	27.303	1.200	30.344	0.382
6.202	1.421	16.442	1.417	21.450	1.409	24.776	1.349	27.378	1.193	30.455	0.329
6.622	1.420	16.762	1.417	21.554	1.408	24.879	1.346	27.448	1.186	30.568	0.282
6.842	1.420	17.082	1.417	21.668	1.408	24.983	1.342	27.521	1.178	30.682	0.234
7.182	1.420	17.402	1.417	21.762	1.407	25.087	1.338	27.594	1.170	30.797	0.187
7.482	1.420	17.722	1.416	21.868	1.406	25.180	1.335	27.687	1.163	30.911	0.139
7.802	1.420	18.042	1.416	21.970	1.405	25.284	1.331	27.740	1.154	31.021	0.094
8.122	1.420	18.362	1.416	22.074	1.404	25.398	1.327	27.813	1.146	31.131	0.048
8.442	1.420	18.682	1.416	22.178	1.403	25.502	1.323	27.805	1.141	31.241	0.002
8.762	1.420	19.002	1.416	22.282	1.402	25.806	1.318	27.916	1.130	31.351	0.000
9.082	1.420	19.061	1.416	22.386	1.400	25.710	1.314	28.032	1.112		

References

1. IEA. *Technology Roadmap-Solar Photovoltaic Energy 2014*; IEA: Paris, France, 2014.
2. Jäger-Waldau, A. Snapshot of photovoltaics February 2018. *EPJ Photovolt.* **2018**, *9*, 6. [CrossRef]
3. Zafrilla Rodríguez, J.E.; Arce Gonzalez, G.; Cadarso Vecina, M.Á.; Córcoles Fuentes, C.; Gómez Sanz, N.; López Santiago, L.A.; Monsalve Serrano, F.; Tobarra Gómez, M.Á. *El Desarrollo Actual de la Energía Solar Fotovoltaica en España*; Universidad de Murcia: Murcia, Spain, 2018.
4. Pandey, A.; Tyagi, V.; Selvaraj, J.A.; Rahim, N.; Tyagi, S. Recent advances in solar photovoltaic systems for emerging trends and advanced applications. *Renew. Sustain. Energy Rev.* **2016**, *53*, 859–884. [CrossRef]
5. Sommerfeld, J.; Buys, L.; Vine, D. Residential consumers' experiences in the adoption and use of solar PV. *Energy Policy* **2017**, *105*, 10–16. [CrossRef]
6. Hussain, A.; Arif, S.M.; Aslam, M. Emerging renewable and sustainable energy technologies: State of the art. *Renew. Sustain. Energy Rev.* **2017**, *71*, 12–28. [CrossRef]
7. Ueckerdt, F.; Brecha, R.; Luderer, G. Analyzing major challenges of wind and solar variability in power systems. *Renew. Energy* **2015**, *81*, 1–10. [CrossRef]
8. Kylili, A.; Fokaides, P.A.; Ioannides, A.; Kalogirou, S. Environmental assessment of solar thermal systems for the industrial sector. *J. Clean. Prod.* **2018**, *176*, 99–109. [CrossRef]
9. Kannan, N.; Vakeesan, D. Solar energy for future world—A review. *Renew. Sustain. Energy Rev.* **2016**, *62*, 1092–1105. [CrossRef]
10. Abolhosseini, S.; Heshmati, A. The main support mechanisms to finance renewable energy development. *Renew. Sustain. Energy Rev.* **2014**, *40*, 876–885. [CrossRef]
11. Zahedi, A. Solar photovoltaic (PV) energy; latest developments in the building integrated and hybrid PV systems. *Renew. Energy* **2006**, *31*, 711–718. [CrossRef]
12. Rauschenbach, H.S. *Solar Cell Array Design Handbook*; J.B. Metzler: Berlin, Germany, 1980.
13. Bandecchi, M.; Melton, B.; Ongaro, F. Concurrent engineering applied to space mission assessment and design. *ESA Bull. Sp. Agency* **1999**, *99*, 34–40.
14. Wall, S.D. Use of Concurrent Engineering in Space Mission Design. In Proceedings of the 2nd European Systems Engineering Conference (EuSEC), Munich, Germany, 13–15 September 2000; pp. 1–6.
15. Braukhane, A.; Quantius, D. Interactions in space systems design within a Concurrent Engineering facility. In Proceedings of the 2011 International Conference on Collaboration Technologies and Systems (CTS), Philadelphia, PA, USA, 23–27 May 2011; pp. 381–388.
16. Ivanov, A.B.; Masson, L.; Belloni, F. Operation of a Concurrent Design Facility for university projects. In Proceedings of the 2016 IEEE Aerospace Conference, Big Sky, MT, USA, 5–12 March 2016; pp. 1–9.
17. Loureiro, G.; Panades, W.; Silva, A. Lessons learned in 20 years of application of Systems Concurrent Engineering to space products. *Acta Astronaut.* **2018**, *151*, 44–52. [CrossRef]
18. Ballesteros, J.B.; Alvarez, J.M.; Arcenillas, P.; Roibas, E.; Cubas, J.; Pindado, S. CDF as a tool for space engineering master's student collaboration and concurrent design learning. In Proceedings of the 8th International Workshop on System & Concurrent Engineering for Space Applications (SECESA 2018), Glasgow, UK, 26–28 September 2018.
19. Roibás-Millán, E.; Sorribes-Palmer, F.; Chimeno-Manguán, M. The MEOW lunar project for education and science based on concurrent engineering approach. *Acta Astronaut.* **2018**, *148*, 111–120. [CrossRef]

20. Cotfas, D.; Cotfas, P.; Kaplanis, S. Methods to determine the dc parameters of solar cells: A critical review. *Renew. Sustain. Energy Rev.* **2013**, *28*, 588–596. [CrossRef]
21. Ortiz-Conde, A.; García-Sánchez, F.J.; Muci, J.; Sucre-González, A. A review of diode and solar cell equivalent circuit model lumped parameter extraction procedures. *Facta Univ. Ser. Electron. Energetics* **2014**, *27*, 57–102. [CrossRef]
22. Jena, D.; Ramana, V.V. Modeling of photovoltaic system for uniform and non-uniform irradiance: A critical review. *Renew. Sustain. Energy Rev.* **2015**, *52*, 400–417. [CrossRef]
23. Chin, V.J.; Salam, Z.; Ishaque, K. Cell modelling and model parameters estimation techniques for photovoltaic simulator application: A review. *Appl. Energy* **2015**, *154*, 500–519. [CrossRef]
24. Humada, A.M.; Hojabri, M.; Mekhilef, S.; Hamada, H.M. Solar cell parameters extraction based on single and double-diode models: A review. *Renew. Sustain. Energy Rev.* **2016**, *56*, 494–509. [CrossRef]
25. Ibrahim, H.; Anani, N. Evaluation of Analytical Methods for Parameter Extraction of PV modules. *Energy Procedia* **2017**, *134*, 69–78. [CrossRef]
26. Abbassi, R.; Abbassi, A.; Jemli, M.; Chebbi, S. Identification of unknown parameters of solar cell models: A comprehensive overview of available approaches. *Renew. Sustain. Energy Rev.* **2018**, *90*, 453–474. [CrossRef]
27. Bader, S.; Ma, X.; Oelmann, B. One-diode photovoltaic model parameters at indoor illumination levels-A comparison. *Sol. Energy* **2019**, *180*, 707–716. [CrossRef]
28. Yang, X.; Gong, W.; Wang, L. Comparative study on parameter extraction of photovoltaic models via differential evolution. *Energy Convers. Manag.* **2019**, *201*, 112113. [CrossRef]
29. Oulcaid, M.; El Fadil, H.; Ammeh, L.; Yahya, A.; Giri, F. Parameter extraction of photovoltaic cell and module: Analysis and discussion of various combinations and test cases. *Sustain. Energy Technol. Assess.* **2020**, *40*, 100736. [CrossRef]
30. Zhang, Y.; Ma, M.; Jin, Z. Comprehensive learning Jaya algorithm for parameter extraction of photovoltaic models. *Energy* **2020**, *211*, 118644. [CrossRef]
31. Li, S.; Gu, Q.; Gong, W.; Ning, B. An enhanced adaptive differential evolution algorithm for parameter extraction of photovoltaic models. *Energy Convers. Manag.* **2020**, *205*. [CrossRef]
32. Ben Messaoud, R. Extraction of uncertain parameters of a single-diode model for a photovoltaic panel using lightning attachment procedure optimization. *J. Comput. Electron.* **2020**, *19*, 1192–1202. [CrossRef]
33. Ridha, H.M.; Gomes, C.; Hizam, H. Estimation of photovoltaic module model's parameters using an improved electromagnetic-like algorithm. *Neural Comput. Appl.* **2020**, *32*, 12627–12642. [CrossRef]
34. Luu, T.V.; Nguyen, N.S. Parameters extraction of solar cells using modified JAYA algorithm. *Optics* **2020**, *203*, 164034. [CrossRef]
35. Abdulrazzaq, A.K.; Bognár, G.; Plesz, B. Evaluation of different methods for solar cells/modules parameters extraction. *Sol. Energy* **2020**, *196*, 183–195. [CrossRef]
36. Gude, S.; Jana, K.C. Parameter extraction of photovoltaic cell using an improved cuckoo search optimization. *Sol. Energy* **2020**, *204*, 280–293. [CrossRef]
37. Yousri, D.; Thanikanti, S.B.; Allam, D.; Ramachandaramurthy, V.K.; Eteiba, M. Fractional chaotic ensemble particle swarm optimizer for identifying the single, double, and three diode photovoltaic models' parameters. *Energy* **2020**, *195*, 116979. [CrossRef]
38. Diab, A.A.Z.; Sultan, H.M.; Do, T.D.; Kamel, O.M.; Mossa, M.A. Coyote Optimization Algorithm for Parameters Estimation of Various Models of Solar Cells and PV Modules. *IEEE Access* **2020**, *8*, 111102–111140. [CrossRef]
39. Liang, J.; Ge, S.; Qu, B.; Yu, K.; Liu, F.; Yang, H.; Wei, P.; Li, Z. Classified perturbation mutation based particle swarm optimization algorithm for parameters extraction of photovoltaic models. *Energy Convers. Manag.* **2020**, *203*, 112138. [CrossRef]
40. Liang, J.; Qiao, K.; Yuan, M.; Yu, K.; Qu, B.; Ge, S.; Li, Y.; Chen, G. Evolutionary multi-task optimization for parameters extraction of photovoltaic models. *Energy Convers. Manag.* **2020**, *207*, 112509. [CrossRef]
41. Long, W.; Cai, S.; Jiao, J.; Xu, M.; Wu, T. A new hybrid algorithm based on grey wolf optimizer and cuckoo search for parameter extraction of solar photovoltaic models. *Energy Convers. Manag.* **2020**, *203*, 112243. [CrossRef]
42. Ridha, H.M.; Heidari, A.A.; Wang, M.; Chen, H. Boosted mutation-based Harris hawks optimizer for parameters identification of single-diode solar cell models. *Energy Convers. Manag.* **2020**, *209*, 112660. [CrossRef]
43. Xiong, G.; Zhang, J.; Shi, D.; Zhu, L.; Yuan, X.; Tan, Z. Winner-leading competitive swarm optimizer with dynamic Gaussian mutation for parameter extraction of solar photovoltaic models. *Energy Convers. Manag.* **2020**, *206*, 112450. [CrossRef]
44. Zhang, Y.; Jin, Z.; Mirjalili, S. Generalized normal distribution optimization and its applications in parameter extraction of photovoltaic models. *Energy Convers. Manag.* **2020**, *224*, 113301. [CrossRef]
45. Montano, J.; Tobón, A.F.; Villegas, J.P.; Durango, M. Grasshopper optimization algorithm for parameter estimation of photovoltaic modules based on the single diode model. *Int. J. Energy Environ. Eng.* **2020**, *11*, 367–375. [CrossRef]
46. Ramadan, A.; Kamel, S.; Korashy, A.; Yu, J. Photovoltaic Cells Parameter Estimation Using an Enhanced Teaching–Learning-Based Optimization Algorithm. *Iran. J. Sci. Technol. Trans. Electr. Eng.* **2019**, *44*, 767–779. [CrossRef]
47. Benahmida, A.; Maouhoub, N.; Sahsah, H. An Efficient Iterative Method for Extracting Parameters of Photovoltaic Panels with Single Diode Model. In Proceedings of the 2020 5th International Conference on Renewable Energies for Developing Countries (REDEC), Marrakech, Morocco, 29–30 June 2020; pp. 1–6.
48. Ndegwa, R.; Simiyu, J.; Ayieta, E.; Odero, N. A Fast and Accurate Analytical Method for Parameter Determination of a Photovoltaic System Based on Manufacturer's Data. *J. Renew. Energy* **2020**, *2020*, 1–18. [CrossRef]

49. Arabshahi, M.; Torkaman, H.; Keyhani, A. A method for hybrid extraction of single-diode model parameters of photovoltaics. *Renew. Energy* **2020**, *158*, 236–252. [CrossRef]
50. Peng, L.; Sun, Y.; Meng, Z.; Wang, Y.; Xu, Y. A new method for determining the characteristics of solar cells. *J. Power Sources* **2013**, *227*, 131–136. [CrossRef]
51. Batzelis, E.I.; Anagnostou, G.; Chakraborty, C.; Pal, B.C. Computation of the Lambert W Function in Photovoltaic Modeling. In *Lecture Notes in Electrical Engineering*; J.B. Metzler: Berlin, Germany, 2020; pp. 583–595.
52. Yu, F.; Huang, G.; Xu, C. An explicit method to extract fitting parameters in lumped-parameter equivalent circuit model of industrial solar cells. *Renew. Energy* **2020**, *146*, 2188–2198. [CrossRef]
53. Ćalasan, M.; Aleem, S.H.A.; Zobaa, A.F. On the root mean square error (RMSE) calculation for parameter estimation of photovoltaic models: A novel exact analytical solution based on Lambert W function. *Energy Convers. Manag.* **2020**, *210*, 112716. [CrossRef]
54. Panchal, A.K. A per-unit-single-diode-model parameter extraction algorithm: A high-quality solution without reduced-dimensions search. *Sol. Energy* **2020**, *207*, 1070–1077. [CrossRef]
55. Nassar-eddine, I.; Obbadi, A.; Errami, Y.; El fajri, A.; Agunaou, M. Parameter estimation of photovoltaic modules using iterative method and the Lambert W function: A comparative study. *Energy Convers. Manag.* **2016**, *119*, 37–48. [CrossRef]
56. Pindado, S.; Cubas, J.; Roibas-Millan, E.; Bugallo-Siegel, F.; Sorribes-Palmer, F. Assessment of Explicit Models for Different Photovoltaic Technologies. *Energies* **2018**, *11*, 1353. [CrossRef]
57. Cubas, J.; Pindado, S.; Victoria, M. On the analytical approach for modeling photovoltaic systems behavior. *J. Power Sour.* **2014**, *247*, 467–474. [CrossRef]
58. Karmalkar, S.; Haneefa, S. A Physically Based ExplicitModel of a Solar Cell for Simple Design Calculations. *IEEE Electron. Device Lett.* **2008**, *29*, 449–451. [CrossRef]
59. Saleem, H.; Karmalkar, S. An Analytical Method to Extract the Physical Parameters of a Solar Cell From Four Points on the Illuminated. *J. Curve. IEEE Electron. Device Lett.* **2009**, *30*, 349–352. [CrossRef]
60. Das, A.K. An explicit J–V model of a solar cell using equivalent rational function form for simple estimation of maximum power point voltage. *Sol. Energy* **2013**, *98*, 400–403. [CrossRef]
61. Cubas, J.; Gomez-Sanjuan, A.M.; Pindado, S. On the thermo-electric modelling of smallsats. In Proceedings of the 50th International Conference on Environmental Systems—ICES 2020, Lisbon, Portugal, 16–20 July 2020; pp. 1–12.
62. Alcala-Gonzalez, D.; Del Toro, E.M.G.; Más-López, M.I.; Pindado, S. Effect of Distributed Photovoltaic Generation on Short-Circuit Currents and Fault Detection in Distribution Networks: A Practical Case Study. *Appl. Sci.* **2021**, *11*, 405. [CrossRef]
63. Pindado, S.; Alcala-Gonzalez, D.; Alfonso-Corcuera, D.; del Toro, E.G.; Más-López, M. Improving the Power Supply Performance in Rural Smart Grids with Photovoltaic DG by Optimizing Fuse Selection. *Agronomy* **2021**, *11*, 622. [CrossRef]
64. Cubas, J.; Pindado, S.; De Manuel, C. Explicit Expressions for Solar Panel Equivalent Circuit Parameters Based on Analytical Formulation and the Lambert W-Function. *Energies* **2014**, *7*, 4098–4115. [CrossRef]
65. Cubas, J.; Pindado, S.; Sanz-Andres, A. Accurate Simulation of MPPT Methods Performance When Applied to Commercial Photovoltaic Panels. *Sci. World J.* **2015**, *2015*, 1–16. [CrossRef]
66. Cubas, J.; Pindado, S.; De Manuel, C. New Method for Analytical Photovoltaic Parameters Identification: Meeting Manufacturer's Datasheet for Different Ambient Conditions. In *Proceedings of the International Congress on Energy Efficiency and Energy Related Materials (ENEFM2013)*; Springer Proceedings in Physics 155; Antalya, Turkey, 9–12 October 2014, Oral, A.Y., Bahsi, Z.B., Ozer, M., Eds.; Springer: Berlin, Germany, 2014; Volume 155, pp. 161–169.
67. Toledo, F.; Blanes, J.M.; Galiano, V.; Laudani, A. In-depth analysis of single-diode model parameters from manufacturer's datasheet. *Renew. Energy* **2021**, *163*, 1370–1384. [CrossRef]
68. Sze, S.M.; Mattis, D.C. Physics of Semiconductor Devices. *Phys. Today* **1970**, *23*, 75. [CrossRef]
69. Van Dyk, E.; Meyer, E. Analysis of the effect of parasitic resistances on the performance of photovoltaic modules. *Renew. Energy* **2004**, *29*, 333–344. [CrossRef]
70. Wolf, M.; Rauschenbach, H. Series resistance effects on solar cell measurements. *Adv. Energy Convers.* **1963**, *3*, 455–479. [CrossRef]
71. Yadir, S.; Bendaoud, R.; El-Abidi, A.; Amiry, H.; BenHmida, M.; Bounouar, S.; Zohal, B.; Bousseta, H.; Zrhaiba, A.; Elhassnaoui, A. Evolution of the physical parameters of photovoltaic generators as a function of temperature and irradiance: New method of prediction based on the manufacturer's datasheet. *Energy Convers. Manag.* **2020**, *203*. [CrossRef]
72. Nguyen-Duc, T.; Nguyen-Duc, H.; Le-Viet, T.; Takano, H. Single-Diode Models of PV Modules: A Comparison of Conventional Approaches and Proposal of a Novel Model. *Energies* **2020**, *13*, 1296. [CrossRef]
73. Humada, A.M.; Darweesh, S.Y.; Mohammed, K.G.; Kamil, M.; Mohammed, S.F.; Kasim, N.K.; Tahseen, T.A.; Awad, O.I.; Mekhilef, S. Modeling of PV system and parameter extraction based on experimental data: Review and investigation. *Sol. Energy* **2020**, *199*, 742–760. [CrossRef]
74. Villalva, M.G.; Gazoli, J.R.; Filho, E.R. Comprehensive Approach to Modeling and Simulation of Photovoltaic Arrays. *IEEE Trans. Power Electron.* **2009**, *24*, 1198–1208. [CrossRef]
75. Villalva, M.G.; Gazoli, J.R.; Filho, E.R. Modeling and circuit-based simulation of photovoltaic arrays. In Proceedings of the 2009 Brazilian Power Electronics Conference, Bonito-Mato Grosso do Sul, Brazil, 27 September–1 October 2009; pp. 1244–1254.
76. Akbaba, M.; Alattawi, M.A. A new model for I–V characteristic of solar cell generators and its applications. *Sol. Energy Mater. Sol. Cells* **1995**, *37*, 123–132. [CrossRef]

77. El Tayyan, A. An Empirical model for Generating the IV Characteristics for a Photovoltaic System. *J. Al Aqsa Univ.* **2006**, *10*, 214–221.
78. El Tayyan, A.A. A simple method to extract the parameters of the single-diode model of a PV system. *Turk. J. Phys.* **2013**, *37*, 121–131. [CrossRef]
79. Das, A.K. An explicit J–V model of a solar cell for simple fill factor calculation. *Sol. Energy* **2011**, *85*, 1906–1909. [CrossRef]
80. Saetre, T.O.; Midtgård, O.-M.; Yordanov, G.H. A new analytical solar cell I–V curve model. *Renew. Energy* **2011**, *36*, 2171–2176. [CrossRef]
81. Pindado, S.; Cubas, J. Simple mathematical approach to solar cell/panel behavior based on datasheet information. *Renew. Energy* **2017**, *103*, 729–738. [CrossRef]
82. Oulcaid, M.; El Fadil, H.; Ammeh, L.; Yahya, A.; Giri, F. One shape parameter-based explicit model for photovoltaic cell and panel. *Sustain. EnergyGrids Netw.* **2020**, *21*, 100312. [CrossRef]
83. Easwarakhanthan, T.; Bottin, J.; Bouhouch, I.; Boutrit, C. Nonlinear Minimization Algorithm for Determining the Solar Cell Parameters with Microcomputers. *Int. J. Sol. Energy* **1986**, *4*, 1–12. [CrossRef]
84. Caillol, J.-M. Some applications of the Lambert W function to classical statistical mechanics. *J. Phys. A Math. Gen.* **2003**, *36*, 10431–10442. [CrossRef]
85. Veberič, D. Lambert W function for applications in physics. *Comput. Phys. Commun.* **2012**, *183*, 2622–2628. [CrossRef]
86. Barry, D.A.; Parlange, J.-Y.; Li, L.; Prommer, H.; Cunningham, C.J.; Stagnitti, F. Analytical approximations for real values of the Lambert W-function. *Math. Comput. Simul.* **2000**, *53*, 95–103. [CrossRef]
87. Cubas, J.; Pindado, S.; Farrahi, A. New method for analytical photovoltaic parameter extraction. In Proceedings of the 2013 International Conference on Renewable Energy Research and Applications (ICRERA), Madrid, Spain, 20–23 October 2013; pp. 873–877.
88. Elkholy, A.; El-Ela, A.A. Optimal parameters estimation and modelling of photovoltaic modules using analytical method. *Heliyon* **2019**, *5*, e02137. [CrossRef] [PubMed]
89. Jadli, U.; Thakur, P.; Shukla, R.D. A New Parameter Estimation Method of Solar Photovoltaic. *IEEE J. Photovolt.* **2018**, *8*, 239–247. [CrossRef]
90. Maouhoub, N. Photovoltaic module parameter estimation using an analytical approach and least squares method. *J. Comput. Electron.* **2018**, *17*, 784–790. [CrossRef]
91. Oliva, D.; El Aziz, M.A.; Hassanien, A.E. Parameter estimation of photovoltaic cells using an improved chaotic whale optimization algorithm. *Appl. Energy* **2017**, *200*, 141–154. [CrossRef]
92. Chin, V.J.; Salam, Z. A New Three-point-based Approach for the Parameter Extraction of Photovoltaic Cells. *Appl. Energy* **2019**, *237*, 519–533. [CrossRef]
93. Swartwout, M. Reliving 24 Years in the Next 12 Minutes: A Statistical and Personal History of University-Class Satellites. In Proceedings of the 32nd AIAA/USU Conference on Small Satellites, Salt Lake City, UT, USA, 4–9 August 2018; pp. 1–20.